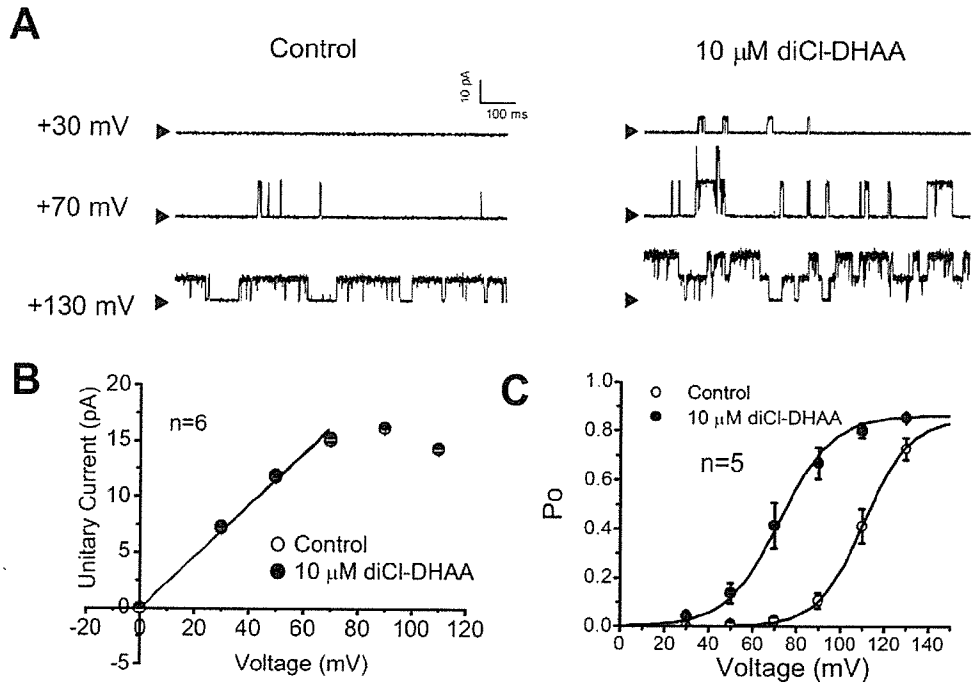

Fig. 5. Effects of diCl-DHAA on single channel conductance and voltage dependence of BKα. Single channel currents of BKα were recorded in inside-out patch configuration at pCa = 7.0 in symmetrical 140 mM K^+ conditions. Recordings were obtained at several test potentials in the range of 0 to +130 mV in the absence and presence of 10 μM diCl-DHAA. Experimental conditions, except applied potentials, are the same as those shown in Fig. 3. A, original current traces at +30, +70, and +130 mV in the absence (left) and presence of 10 μM diCl-DHAA (right). B, relationship between unitary current amplitude and test potentials was plotted in a range of 0 and +70 mV in the absence (open circles) and presence of 10 μM diCl-DHAA (closed circles) and was fitted by a linear line. The single channel conductance was determined from the slope (n = 6). C, effects of diCl-DHAA on voltage dependence of BKα. The relationships between P_o and test potentials were obtained in the absence (open circles) and presence of 10 μM diCl-DHAA (closed circles). Number of examples is five for each. The data were fitted using the Boltzmann equation (see "Results"). The fitted lines are based on the following values of $V_{1/2}$, S, and C: 110.7 mV, 10.5 mV, and 0.15 in the absence and 72.3 mV, 12.2 mV, and 0.13 in the presence of 10 μM diCl-DHAA, respectively.

current amplitude (10.43 ± 0.28 pA, 0.0180 ± 0.0047, n = 6; Fig. 3, A and B). It is notable that diCl-DHAA was effective on BKα even when applied to the cytosolic phase. This effect of diCl-DHAA was completely removed by the washout. The P_o was significantly increased by diCl-DHAA at 0.3 μM and higher concentrations (Fig. 3C), and the relative P_o determined by taking P_o in the control as unity was 1.26 ± 0.13, 1.92 ± 0.19, 6.24 ± 0.67, and 14.45 ± 1.72 in the presence of 0.1, 0.3, 1.0, and 3.0 μM diCl-DHAA, respectively (n = 4–6). These results are mostly comparable with those obtained under whole-cell clamp conditions (Fig. 1C). In Fig. 4, the potency of diCl-DHAA to activate BKα was compared with that of abietic acid and dehydroabietic acid, an aromatic derivative of abietic acid. The data for pimaric acid, a potent BK channel opener, were also taken from a previous study, where the potency of pimaric acid was determined under the same experimental conditions (Imaizumi et al., 2002). Even a high concentration of abietic acid at 30 and 100 μM failed to increase the activity of BKα, whereas dehydroabietic acid at 3 and 10 μM increased activity significantly. Nevertheless, diCl-DHAA was much more potent as an activator of BKα than dehydroabietic acid and pimaric acid.

Effects of diCl-DHAA on Characteristics of Single BKα Channel Currents. In Fig. 5, effects of diCl-DHAA on characteristics of single BKα channel currents were systematically examined in the excised inside-out patch configuration. The bathing and pipette solution contained symmetrical 140 mM K^+. The pCa in the bathing solution was 7. The conductance of BKα, which was determined by slope of the regression line between 0 and +70 mV, was 224.8 ± 4.1 and 224.8 ± 4.3 pS in the absence and presence of 10 μM diCl-DHAA, respectively (n = 6; $p > 0.05$; Fig. 5B), indicating that diCl-DHAA did not affect BKα channel conductance. The inward rectification shown at high potentials (more than +80 mV) was consistent with that reported as voltage-dependent block of BK channel by Na^+ (Yellen, 1984) and was not affected by diCl-DHAA. Moreover, the P_o in the absence and presence of 10 μM diCl-DHAA was calculated and plotted against test potentials in Fig. 5C. Under these conditions, the increase in P_o was voltage-dependent in the range of +30 to +130 mV, and a set of data were well described by Boltzmann relationship:

$$P_o = (1 - C)/[1 + \exp\{(V_{1/2} - V_m)/S\}] \quad (1)$$

where $V_{1/2}$, V_m, S, and C is the voltage required for half-maximum activation, membrane potential, slope factor, and constant, respectively. Application of 10 μM diCl-DHAA neither changed S nor C (S, 10.5 ± 1.5 and 12.2 ± 1.3 mV; C, 0.15 ± 0.03 and 0.13 ± 0.02 in the absence and presence of diCl-DHAA, respectively; n = 5), whereas it significantly shifted $V_{1/2}$ to a more negative potential (110.7 ± 3.3 and 72.4 ± 5.7mV, respectively; n = 5; $p < 0.01$).

In Fig. 6, the effects of diCl-DHAA on Ca^{2+} sensitivity of BKα were examined at 0 mV in asymmetrical 5.9/140 mM K^+ conditions. When Ca^{2+} concentration in the bathing solution was elevated in a pCa range between 7.0 and 5.0, the P_o was increased in a concentration-dependent manner (Fig. 6, A and B). The relationship between Ca^{2+} concentration and the P_o of BKα was fitted by the following equation:

$$P_o = (1 - C)/1 + (K_d/[Ca^{2+}]_i)^m \quad (2)$$

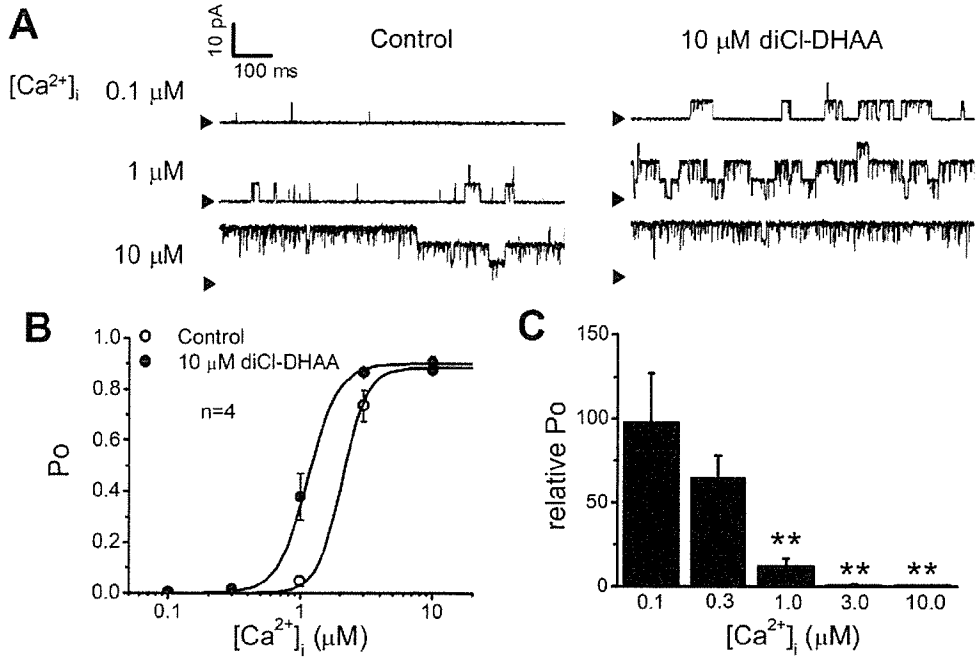

Fig. 6. Effects of diCl-DHAA on Ca^{2+} dependence of BKα. A, single channel currents of BKα were recorded in inside-out patch configuration at 0 mV in asymmetrical K^+ conditions (5.9/140 mM K^+) in the absence and presence of 10 μM diCl-DHAA. Recordings were obtained when $[Ca^{2+}]_i$ was 0.1, 1, or 10 μM. B, relationships between P_o and $[Ca^{2+}]_i$ were obtained in the absence (open circles) and presence of 10 μM diCl-DHAA (closed circles). Number of examples is four for each experiment. The data were fitted with the Hill equation (see *Results*). The fitted lines were plotted based on the following values of K_d, m, and C: 2.06, 4.65, and 0.15μM in the absence and 1.14, 3.83, and 0.10 μM in the presence of 10 μM diCl-DHAA, respectively. C, relative P_o in the presence of 10 μM diCl-DHAA versus that in the absence of 10 μM diCl-DHAA was re-evaluated at various $[Ca^{2+}]_i$ from the data shown in B. **, $p < 0.01$ versus relative P_o at 0.1 μM Ca^{2+}.

where K_d is an apparent dissociation constant of Ca^{2+}, $[Ca^{2+}]_i$ is the pCa in the bathing solution, m is a Hill coefficient, and C is a constant. Under the control conditions, K_d, m, and C, which were obtained from the best fitting, were pCa = 5.68 ± 0.03, 4.65 ± 0.92, and 0.152 ± 0.029, respectively (n = 4). In the presence of 10 μM diCl-DHAA, K_d was changed to pCa = 5.94 ± 0.03 (n = 4; $p < 0.05$), whereas the Hill coefficient, which indicates binding of one Ca^{2+} to each α subunit in the tetrameric complex of a functional BKα channel, was not significantly affected (3.83 ± 0.45; $p > 0.05$ versus control). C was 0.102 ± 0.008 and not affected by diCl-DHAA ($p > 0.05$ versus control). The relative P_o in the presence of 10 μM diCl-DHAA to that of the control was plotted against $[Ca^{2+}]_i$ in Fig. 6C. The lower the P_o in the control conditions, the larger the enhancement by diCl-DHAA.

Effects of diCl-DHAA on the kinetic properties of BKα were examined in excised inside-out patches, which included only one channel (Fig. 7). These patches had a single channel event even when $[Ca^{2+}]_i$ was elevated to pCa = 3.5. Figure 7A shows original current traces of BKα at pCa = 6.5 in the absence and presence of 10 μM diCl-DHAA. The data for open and closed dwell time in Fig. 7A were reconstituted as distribution histograms in Fig. 7, B and C, respectively. These histograms were well fitted by a double and triple exponential function, respectively (Fig. 7, B and C). As shown in Table 1, application of 10 μM diCl-DHAA caused a marked decrease in the mean closed time (τ_{Cs}) and its relative magnitude (A_{Cs}) of the slow component (4–5 times change), whereas other parameters were moderately changed (τ_{Os}, τ_{Cf}, τ_{Ci}, and A_{Of}) or were not affected (τ_{Of}, A_{Os}, A_{Cf}, and A_{Ci}) (n = 5).

Comparison of diCl-DHAA-Induced Effects on BKα with Those on BK$\alpha\beta$1. The enhancement of single BKα channel activity by diCl-DHAA indicated the direct action of this compound on BKα. It has been, however, established that coexpression of β1 subunit with BKα increases the sensitivity of BKα to Ca^{2+} and voltage (Wallner et al., 1996; Cox

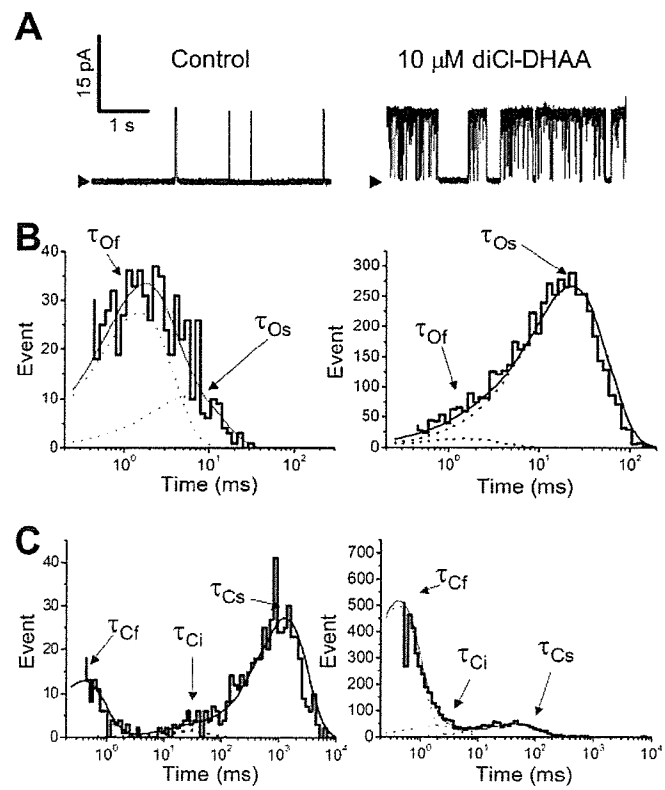

Fig. 7. Kinetics of diCl-DHAA-induced activation of BKα. A, single channel currents of BKα were recorded at +50 mV in inside-out patch configuration at pCa = 6.5 in symmetrical 140 mM K^+ conditions. B, dwell-time histograms of open times before (left) and after (right) application of 10 μM diCl-DHAA. The open-time histogram in the absence and presence of diCl-DHAA was fitted by a double exponential function. τ_{Of} and τ_{Os} represent time constants of the fast and slow components of the open times in BKα kinetics, respectively. Continuous lines show the sum of individual components (dotted lines). C, dwell-time histograms of closed times before (left) and after (right) application of 10 μM diCl-DHAA. The closed time histogram was fitted by a triple exponential function. τ_{Cf}, τ_{Ci}, and τ_{Cs} represent time constants of the fast, intermediate, and slow components of closed times, respectively.

and Aldrich, 2000). To determine whether diCl-DHAA also acts on the functional coupling between BKα and β1 subunits, the increase in P_o by diCl-DHAA in BK$\alpha\beta$1 was compared with that in BKα in inside-out patches. The P_o of BKα at pCa = 7.0 was increased at any test potential by coexpression with β1 subunit (Fig. 8A). Since the increase in P_o by diCl-DHAA depended on a basal P_o before application (Fig. 6C), effects of diCl-DHAA on BKα at +40 mV were compared with those on BK$\alpha\beta$1 at +20 mV. The basal P_o values were comparable with each other (0.0028 ± 0.0006 versus 0.0023 ± 0.0006; n = 5; Fig. 8B). The application of 1 μM diCl-DHAA increased the P_o to 0.0180 ± 0.0058 in BKα (n = 5; $p < 0.05$) and to 0.0208 ± 0.0037 in BK$\alpha\beta$1 (n = 5; $p < 0.01$). The ratio of P_o in BKα in the presence and absence of diCl-DHAA was 7.2 ± 0.8 and therefore not significantly different from that in BK$\alpha\beta$1 (11.1 ± 3.1; $p > 0.05$). This finding strongly suggests that coexpression of β1 subunit did not affect the diCl-DHAA-induced enhancement of BKα.

Selectivity of diCl-DHAA on BK Channel Versus Voltage-Dependent Ca^{2+} Channel. To examine whether the action of diCl-DHAA is selective to BK channels over CaV channels, effects of 0.3 and 1 μM diCl-DHAA on BKα were compared with those on CaV channel currents in HEK293 cells, which coexpressed α1 subunit of rabbit CaV channel and β3 subunit of mouse CaVα1Cβ3. Here, effects of pimaric acid on CaVα1Cβ3 were also examined. The inward currents through CaVα1Cβ3 were elicited upon depolarization from a holding potential of −60 mV to test potentials in a range of −50 and +40 mV by 10-mV step every 10 s. The maximum amplitude was obtained at +10 mV (peak amplitude, 193 ± 54.4 pA; n = 6; Fig. 9A). CaVα1Cβ3 channel currents were not inhibited by 0.3 μM diCl-DHAA or pimaric acid, whereas they were significantly inhibited by both compounds at 1 μM (only diCl-DHAA; Fig. 9A). Data about effects of diCl-DHAA and pimaric acid on BKα are those shown in Fig. 3 and provided in a previous study (Imaizumi et al., 2002) and were obtained in inside-out patches at +40 mV and pCa = 7.0 under symmetrical 140 mM K^+ conditions. Enhancement of BK channel activity by diCl-DHAA was significant at 0.3 and 1 μM, indicating that 0.3 μM diCl-DHAA is selective for the BK channel over the CaV channel.

TABLE 1
Time constants and relative weights

	Control	diCl-DHAA	diCl-DHAA/ Control
Time constants (ms)			
τ_{Of}	1.49 ± 0.17	1.53 ± 0.22	1.02 ± 0.10
τ_{Os}	10.34 ± 3.75	23.73 ± 5.38	2.68 ± 0.52*
τ_{Cf}	0.65 ± 0.05	0.74 ± 0.04	1.14 ± 0.04*
τ_{Ci}	43.32 ± 11.05	11.33 ± 3.96	0.41 ± 0.16*
τ_{Cs}	1955.19 ± 560.17	264.08 ± 77.97	0.21 ± 0.07**
Relative weights			
A_{Of}	0.53 ± 0.11	0.16 ± 0.04	0.40 ± 0.12**
A_{Os}	0.47 ± 0.11	0.84 ± 0.04	2.15 ± 0.44
A_{Cf}	0.40 ± 0.08	0.82 ± 0.02	2.43 ± 0.54
A_{Ci}	0.12 ± 0.04	0.11 ± 0.01	1.74 ± 0.73
A_{Cs}	0.44 ± 0.11	0.07 ± 0.02	0.23 ± 0.07**

* $p < 0.05$ and ** $p < 0.01$ vs. unity (n = 5).

Discussion

In the present study, we have demonstrated that diCl-DHAA is one of the most potent synthesized activators affecting the BKα subunit via changing the voltage and Ca^{2+} sensitivity of the channel. Chemical modification of abietic acid, an inactive compound, to dehydroabietic acid and diCl-DHAA provides a potent and selective BK channel opener. The latter has an inverse voltage dependence for BKα channel activation and is one of the most potent openers available by application from outside of the cell membrane.

BK channels consist of channel-forming α subunits and accessory β subunits (β1–β4) arranged in tetramers (Vergara et al., 1998). Each β subunit interacts with N-terminal region of an α subunit (Wallner et al., 1996) and regulates the activity of the α subunit by changing Ca^{2+} and voltage sensitivity and/or channel kinetics. Although only one major type of α subunit with splice variants has been defined, the combination of the BK channel α subunit encoded by KCNMA1 and β subunits encoded by KCNMB1-4 provides the

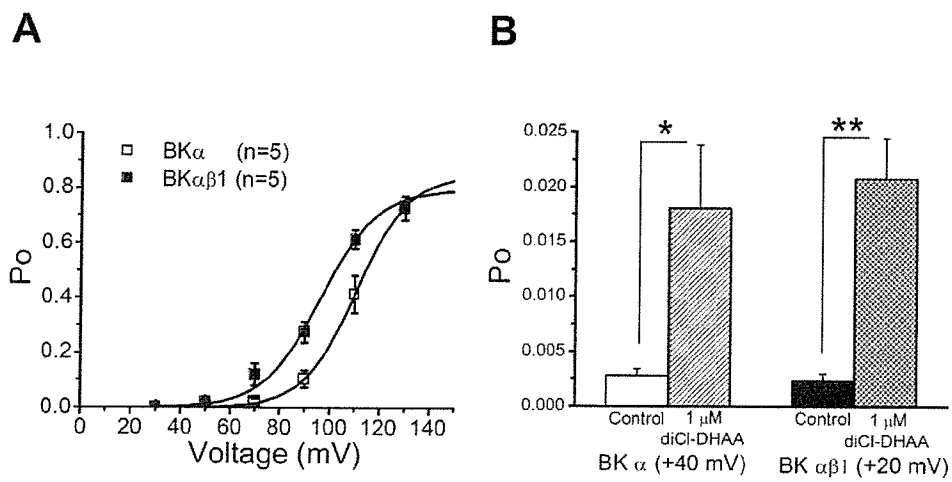

Fig. 8. Comparison of effects of diCl-DHAA on single channel currents due to BKα or BK$\alpha\beta$1. A, relationships between P_o and test potentials were obtained in HEKBKα (open squares) and HEKBK$\alpha\beta$1 (closed squares). Recordings were obtained at pCa = 7.0 in symmetrical 140 mM K^+ conditions. Number of examples is five for each experiment. The data were fitted using the Boltzmann equation (see *Results*). The fitted lines are based on the following values of $V_{1/2}$, S, and C: 110.7 mV, 10.5 mV, and 0.15 in HEKBKα and 96.3 mV, 11.4 mV, and 0.20 in HEKBK$\alpha\beta$1, respectively. B, effect of 1 μM diCl-DHAA on P_o of BK$\alpha\beta$1 was compared with that of BKα. The P_o of BKα in the absence of diCl-DHAA was 0.00382 ± 0.00104 at +40 mV and close to P_o of BK$\alpha\beta$1 at +20 mV (0.00346 ± 0.00079; $p > 0.05$). Number of examples is five for each. *, $p < 0.05$ and **, $p < 0.01$ versus the corresponding control.

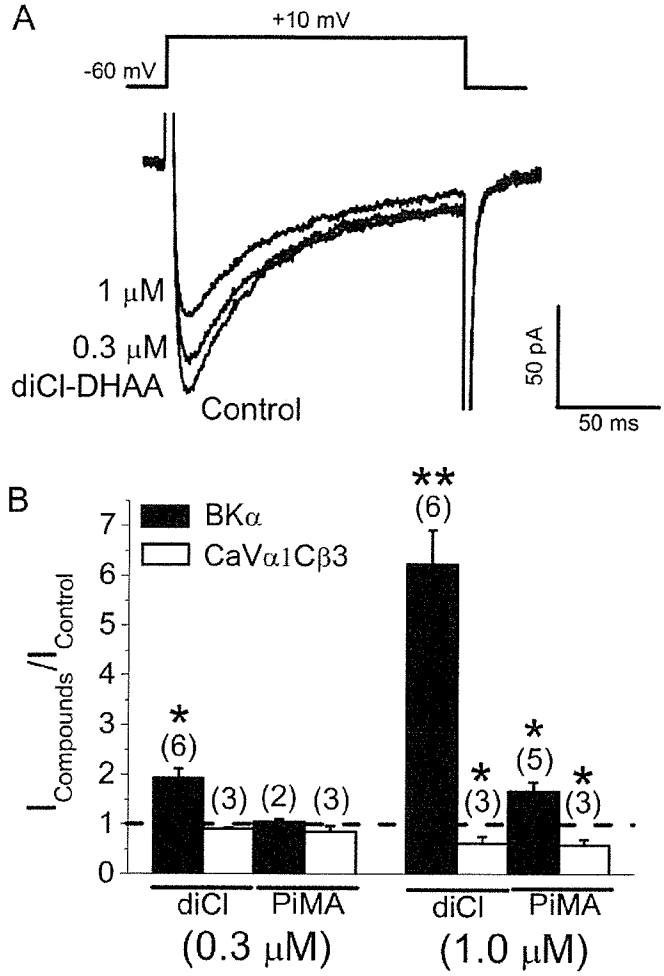

Fig. 9. Inhibitory effects of diCl-DHAA and pimaric acid on CaV channel currents. A, representative current traces obtained from HEKs coexpressing rabbit α1C and mouse β3 with GFP (see *Materials and Methods*). The inward currents were elicited by 150-ms depolarizing pulses to +10 mV from a holding potential of −60 mV in the absence and presence of 0.3 or 1 μM diCl-DHAA. B, summary of effects of diCl-DHAA and pimaric acid on CaV channel currents (closed columns). For comparison, their effects on BKα are also illustrated. Inhibitory effects of diCl-DHAA and pimaric acid on CaV channel currents were examined in experiments identical to that shown in A, and the relative amplitude of inward currents at +10 mV in the presence of each compound was determined taking the amplitude in the absence as unity. For revaluation of effects of diCl-DHAA and pimaric acid on BKα, the same set of data shown in Fig. 3 (present study) and Fig. 5 (Imaizumi et al., 2002) were used. Means ± S.E.M. are shown by columns and vertical bars, respectively. The number in parenthesis denotes number of cells used. *, $p < 0.05$ and **, $p < 0.01$ versus unity.

diversity of BK channels (McManus et al., 1995; Brenner et al., 2000a; Uebele et al., 2000), which offers opportunities of development of new therapeutic agents. Benzimidazolone derivatives such as biarylureas (NS-1608), NS-1619, BMS-204352 (Gribkoff et al., 2001), arylpyrrole (NS-8), and indole-3-carboxylic acid esters (CGS-7181 and CGS-7184) have been characterized as effective BK channel openers (Coghlan et al., 2001).

Natural products have also been evaluated as BK channel openers, and terpenoids such as dehydrosoyasaponin I (McManus et al., 1993), maxikdiol (Singh et al., 1994), and L-735,334 (Lee et al., 1995) have been identified as active BK channel openers. Our pioneer work of pimarane compounds, which have a close structural similarity to maxikdiol, has revealed that pimaric acid is a potent BK channel opener that interacts with BKα subunit but not with the BKβ1 subunit (Imaizumi et al., 2002). Pimaric acid activates BK channels in HEKBK$\alpha\beta$1 when applied externally as well as when applied to the "internal phase" in inside-out patches. Its potency seems to be slightly higher than that of maxikdiol. An important comparative result in the previous study is that abietic acid did not show BK channel opening action despite of the fact that abietic acid is a structural isomer ($C_{20}H_{30}O_2$) of pimaric acid.

Of importance is our recent finding that chemical modification of abietic acid to dehydroabietic acid as well as diCl-DHAA produced compounds active to the open BK channel (Ohwada et al., 2003). In the present study, we provided new information about mechanisms of diCl-DHAA-induced activation of BK channels. diCl-DHAA activated BK channels in HEKBKα when applied externally as well as when applied to the internal phase in inside-out patches. Its potency was obviously higher than that of pimaric acid in whole-cell recording under the same experimental conditions, since significant activation was observed at 0.1 μM diCl-DHAA (Imaizumi et al., 2002). Dehydrosoyasaponin-I (Giangiacomo et al., 1998), 17β-estradiol (Valverde et al., 1999), and tamoxifen (Dick et al., 2001) interact with β subunits of BK channels to increase the channel activity. In contrast, NS-1619 (Ahring et al., 1997), epoxyeicosatrienoic acid (Fukao et al., 2001), Evans blue (Yamada et al., 2001), and pimaric acid (Imaizumi et al., 2002) act on the BKα subunit. Our results clearly showed that diCl-DHAA interacts with the BKα subunit but may not interact with the BKβ1 subunit. We also found that 100 nM iberiotoxin completely removed the diCl-DHAA-induced potentiation of the macroscopic BK$\alpha\beta$1 channel currents. This finding suggests that diCl-DHAA does not affect the iberiotoxin binding to BK$\alpha\beta$1, although effects of diCl-DHAA on ^{125}I-iberiotoxin binding were not examined in this study. Consistently, the concentration-response relationship of charybdtoxin for the inhibition of macroscopic BK$\alpha\beta$1 channel currents was not affected by the presence of 10 μM pimaric acid, which has a close structural analogy to diCl-DHAA (Imaizumi et al., 2002).

It is obvious from the present results that diCl-DHAA activates BK channels in a voltage- and Ca^{2+}-dependent manner. It is very notable that the potentiation of BK channel activity by diCl-DHAA was significantly larger at negative potentials as well as at lower Ca^{2+} concentrations. In contrast, BMS-204352, a potent BK channel opener, caused activation of BK channel currents only at positive potentials (more than +30 mV; Gribkoff et al., 2001; Schrøder et al., 2003). To our knowledge, diCl-DHAA, and presumably pimaric acid as well, are the only compounds that show marked inversed voltage dependence for potentiation among various types of BK channel openers. This characteristic feature of diCl-DHAA can be considered particularly effective to prevent membrane depolarization, hyperexcitability, and/or excess Ca^{2+} influx to the cell and may be advantageous for clinical use. Moreover, diCl-DHAA decreased the time for the channels to stay in the prolonged closed states. It can be, therefore, suggested that this kinetic change in the presence of diCl-DHAA causes activation of BK channel. Niflumic acid opens BK channels mainly by decreasing the time in the long-closed states (Ottolia and Toro, 1994).

It is important to characterize the selectivity of diCl-DHAA to BK channels over that of other ion channels. We found that diCl-DHAA at concentrations of 0.3 μM or less increased BK channel activity without inhibiting CaV channels. Moreover, even though diCl-DHAA-induced inhibition of CaV channels at 1 μM was comparable with that by 1 μM pimaric acid (~30% of the control), the activation of BK channel currents by diCl-DHAA was significantly greater than that by pimaric acid, suggesting that the potent activation of BK channels by diCl-DHAA provides more selectivity against CaV channels than that by pimaric acid. The selectivity of BK channel openers against CaV channels has not been well defined, but nordihydroguaiaretic acid or NS-1619-induced inhibition of CaV channel currents was comparable with or slightly more potent than the activation of BK channels, respectively (Holland et al., 1996; Yamamura et al., 1999). For development of potent and selective BK channel openers, scaffoldings of dehydroabietic acid may be useful (Ohwada et al., 2003).

Effects of diCl-DHAA on small (SK) and intermediate (IK) conductance Ca^{2+}-activated K^+ channels were not examined systematically in this study. BK channel openers reported so far, including pimaric acid, are however selective over SK and IK channels (Kaczorowski and Garcia, 1999; Coghlan et al., 2001; Imaizumi et al., 2002), and our preliminary data suggest that 1 μM diCl-DHAA did not affect the activities of SK2 and SK4 channels (K. Sakamoto, unpublished data). Genetically, and even functionally in some aspects, KCNMA (BK) is closer to voltage-dependent K^+ channels than KCNN (SK and IK), because of the presence of its voltage-sensitive domain (Vergara et al., 1998). It is therefore worth examining the effects of diCl-DHAA on cloned voltage-dependent K^+ channels, which remain to be determined.

In conclusion, our results provide new information of mechanisms underlying diCl-DHAA-induced activation of BK channels and the selectivity against CaV channels. diCl-DHAA is effective from either side of cell membrane and acts on BKα subunit to increase Ca^{2+} and voltage sensitivity. In contrast to many other BK channel openers, the effect of diCl-DHAA on BKα significantly showed inverse voltage dependence, i.e., larger potentiation at lower membrane potentials. In this respect, diCl-DHAA may be one of the most potent BK channel openers ever known to sensitize the negative feedback control of $[Ca^{2+}]_i$ regulation via activation of BK channels, which suppress depolarization from resting membrane potential, and subsequently, membrane excitability. diCl-DHAA at low concentrations (<1 μM) shows selectivity to the BK channel over CaV channels and possesses higher selectivity to BK channels than pimaric acid. Dehydroabietic acid, including diCl-DHAA, is a new prototype scaffolding as a potent BKα channel opener.

Acknowledgments

We thank Dr. Wayne Giles (University of Calgary, Calgary, AB, Canada) for providing data acquisition and analysis programs for macroscopic current analyses and also for critical reading of this manuscript. We also thank Dr. John Dempster (University of Strathclyde) for providing data acquisition and analysis programs for single channel analyses.

References

Ahring PK, Strobaek D, Christophersen P, Olesen SP, and Johansen TE (1997) Stable expression of the human large-conductance Ca^{2+}-activated K^+ channel α- and β-subunits in HEK293 cells. *FEBS Lett* **415**:67–70.

Bolton TB and Imaizumi Y (1996) Spontaneous transient outward currents in smooth muscle cells. *Cell Calcium* **20**:141–152.

Brenner R, Jegla TJ, Wickenden A, Liu Y, and Aldrich RW (2000a) Cloning and functional characterization of novel large conductance calcium-activated potassium channel β subunits, hKCNMB3 and hKCNMB4. *J Biol Chem* **275**:6453–6461.

Brenner R, Perez GJ, Bonev AD, Eckman DM, Kosek JC, Wiler SW, Patterson AJ, Nelson MT, and Aldrich RW (2000b) Vasoregulation by the β1 subunit of the calcium-activated potassium channel. *Nature (Lond)* **407**:870–876.

Coghlan MJ, Carroll WA, and Gopalakrishnan M (2001) Recent developments in the biology and medicinal chemistry of potassium channel modulators: update from a decade of progress. *J Med Chem* **44**:1627–1653.

Cox DH and Aldrich RW (2000) Role of the beta1 subunit in large-conductance Ca(2+)-activated K(+) channel gating energetics. Mechanisms of enhanced Ca(2+) sensitivity. *J Gen Physiol* **116**:411–432.

Dick GM, Rossow CF, Smirnov S, Horowitz B, and Sanders KM (2001) Tamoxifen activates smooth muscle BK channels through the regulatory β1 subunit. *J Biol Chem* **276**:34594–34599.

Fernández-Fernández JM, Tomas M, Vazquez E, Orio P, Latorre R, Senti M, Marrugat J, and Valverde MA (2004) Gain-of-function mutation in the KCNMB1 potassium channel subunit is associated with low prevalence of diastolic hypertension. *J Clin Investig* **113**:1032–1039.

Fukao M, Mason HS, Kenyon JL, Horowitz B, and Keef KD (2001) Regulation of BKCa channels expressed in human embryonic kidney 293 cells by epoxyeicosatrienoic acid. *Mol Pharmacol* **59**:16–23.

Giangiacomo KM, Kamassah A, Harris G, and McManus OB (1998) Mechanism of maxi-K channel activation by dehydrosoyasaponin-I. *J Gen Physiol* **112**:485–501.

Gribkoff VK, Starrett JE Jr, Dworetzky SI, Hewawasam P, Boissard CG, Cook DA, Frantz SW, Heman K, Hibbard JR, Huston K, et al. (2001) Targeting acute ischemic stroke with a calcium-sensitive opener of maxi-K potassium channels. *Nat Med* **7**:471–477.

Holland M, Langton PD, Standen NB, and Boyle JP (1996) Effects of the BK_{Ca} channel activator, NS1619, on rat cerebral artery smooth muscle. *Br J Pharmacol* **117**:119–129.

Imaizumi Y, Muraki K, and Watanabe M (1989) Ionic currents in single smooth muscle cells from the ureter of the guinea-pig. *J Physiol (Lond)* **411**:131–159.

Imaizumi Y, Ohi Y, Yamamura H, Ohya S, Muraki K, and Watanabe M (1999) Ca^{2+} spark as a regulator of ion channel activity. *Jpn J Pharmacol* **80**:1–8.

Imaizumi Y, Sakamoto K, Yamada A, Hotta A, Ohya S, Muraki K, Uchiyama M, and Ohwada T (2002) Molecular basis of pimarane compounds as novel activators of large-conductance Ca^{2+}-activated K^+ channel α-subunit. *Mol Pharmacol* **62**:836–846.

Imaizumi Y, Torii Y, Ohi Y, Nagano N, Atsuki K, Yamamura H, Muraki K, Watanabe M, and Bolton TB (1998) Ca^{2+} images and K^+ current during depolarization in smooth muscle cells of the guinea-pig vas deferens and urinary bladder. *J Physiol (Lond)* **510**:705–719.

Kaczorowski GJ and Garcia ML (1999) Pharmacology of voltage-gated and calcium-activated potassium channels. *Curr Opin Chem Biol* **3**:448–458.

Lawson K (2000) Potassium channel openers as potential therapeutic weapons in ion channel disease. *Kidney Int* **57**:838–845.

Lee SH, Hensens OD, Helms GL, Liesch JM, Zink DL, Giacobbe RA, Bills GF, Stevens-Miles S, Garcia ML, and Schmalhofer WA (1995) L-735,334, a novel sesquiterpenoid potassium channel-agonist from *Trichoderma virens*. *J Nat Prod* **58**:1822–1828.

McManus OB, Harris GH, Giangiacomo KM, Feigebaum P, Reuben JP, Addy ME, Burka JF, Kaczorowski GJ, and Garcia ML (1993) An activator of calcium-dependent potassium channels isolated from a medicinal herb. *Biochemistry* **32**: 6128–6133.

McManus OB, Helms LM, Pallanck L, Ganetzky B, Swanson R, and Leonard RJ (1995) Functional role of the beta subunit of high conductance calcium-activated potassium channels. *Neuron* **14**:645–650.

Murakami M, Yamamura H, Suzuki T, Kang M, Ohya S, Murakami A, Miyoshi I, Sasano H, Muraki K, Hano T, et al. (2003) Modified cardiovascular L-type channels in mice lacking the voltage-dependent Ca^{2+} channel β3 subunit. *J Biol Chem* **278**:43261–43267.

Nelson MT and Quayle JM (1995) Physiological roles and properties of potassium channels in arterial smooth muscle. *Am J Physiol* **268**:C799–C822.

Ohi Y, Yamamura H, Nagano N, Ohya S, Muraki K, Watanabe M, and Imaizumi Y (2001) Local Ca^{2+} transients and distribution of BK channels and ryanodine receptors in smooth muscle cells of guinea-pig vas deferens and urinary bladder. *J Physiol (Lond)* **534**:313–326.

Ohwada T, Nonomura T, Maki K, Sakamoto K, Ohya S, Muraki K, and Imaizumi Y (2003) Dehydroabietic acid derivatives as a novel scaffold for large-conductance calcium-activated K^+ channel openers. *Bioorg Med Chem Lett* **13**:3971–3974.

Ottolia M and Toro L (1994) Potentiation of large conductance K_{Ca} channels by niflumic, flufenamic and mefenamic acids. *Biophys J* **67**:2272–2279.

Schroder RL, Strobaek D, Olesen SP, and Christophersen P (2003) Voltage-independent KCNQ4 currents induced by (±)BMS-204352. *Pflueg Arch Eur J Physiol* **446**:607–616.

Singh SB, Goetz MA, Zink DL, Dombrowski AW, Polishook JD, Garcia ML, Schmalhofer W, McManus OB, and Kaczorowski GJ (1994) Maxikdiol: a novel dihydroxyisoprimane as an agonist of maxi-K channels. *J Chem Soc Perkin Trans* **1**:3349–3352.

Uebele VN, Lagrutta A, Wade T, Figueroa DJ, Liu Y, McKenna E, Austin CP, Bennett PB, and Swanson R (2000) Cloning and functional expression of two families of beta-subunits of the large conductance calcium-activated K^+ channel. *J Biol Chem* **275**:23211–23218.

Valverde MA, Rojas P, Amigo J, Cosmelli D, Orio P, Bahamonde MI, Mann GE, Vergara C, and Latorre R (1999) Acute activation of maxi-K channels (hSlo) by estradiol binding to the β subunit. *Science (Wash DC)* **285**:1929–1931.

Vergara C, Latorre R, Marrion NV, and Adelman JP (1998) Calcium-activated potassium channels. *Curr Opin Neurobiol* **8**:321–329.

Wallner M, Meera P, and Toro L (1996) Determinant for β-subunit regulation in high-conductance voltage-activated and Ca^{2+}-sensitive K^+ channels: an additional transmembrane region at the N terminus. *Proc Natl Acad Sci USA* **93**:14922–14927.

Wellman GC and Nelson MT (2003) Signaling between SR and plasmalemma in smooth muscle: sparks and the activation of Ca^{2+} sensitive ion channels. *Cell Calcium* **34**:211–229.

Yamada A, Gaja N, Ohya S, Muraki K, Narita H, Ohwada T, and Imaizumi Y (2001) Usefulness and limitation of $DiBAC_4(3)$, a voltage-sensitive fluorescent dye, for the measurement of membrane potentials regulated by recombinant large conductance Ca^{2+}-activated K^+ channels in HEK293 cells. *Jpn J Pharmacol* **86**:342–350.

Yamamura H, Nagano N, Hirano M, Muraki K, Watanabe M, and Imaizumi Y (1999) Activation of Ca^{2+}-dependent K^+ current by nordihydroguaiaretic acid in porcine coronary arterial smooth muscle cells. *J Pharmacol Exp Ther* **291**: 140–146.

Yellen G (1984) Ionic permeation and blockade in Ca^{2+}-activated K^+ channels of bovine chromaffin cells. *J Gen Physiol* **84**:157–186.

Address correspondence to: Dr. Yuji Imaizumi, Department of Molecular and Cellular Pharmacology, Graduate School of Pharmaceutical Sciences, Nagoya City University, 3-1 Tanabedori, Mizuhoku, Nagoya 467-8603, Japan. E-mail: yimaizum@phar.nagoya-cu.ac.jp

BRAIN RESEARCH XX (2007) XXX–XXX

available at www.sciencedirect.com

ScienceDirect

www.elsevier.com/locate/brainres

BRAIN RESEARCH

Research Report

β-Estradiol induces synaptogenesis in the hippocampus by enhancing brain-derived neurotrophic factor release from dentate gyrus granule cells

Kaoru Sato[a,*], *Tatsuhiro Akaishi*[b], *Norio Matsuki*[c], *Yasuo Ohno*[a], *Ken Nakazawa*[a]

[a]*Division of Pharmacology, National Institute of Health Sciences, 1-18-1 Kamiyoga, Setagaya-ku, Tokyo 158-8501, Japan*
[b]*Laboratory of Pharmacology, Faculty of Pharmacy and Research Institute of Pharmaceutical Sciences, Musashino University, 1-1-20 Shinmachi, Nishitokyo-shi, Tokyo 202-8585, Japan*
[c]*Laboratory of Chemical Pharmacology, Graduate School of Pharmaceutical Sciences, University of Tokyo, 7-3-1 Hongo, Bunkyo-ku, Tokyo 113-0033, Japan*

ARTICLE INFO

Article history:
Accepted 28 February 2007

Keywords:
β-Estradiol
Organotypic hippocampal slice culture
Dentate gyrus
CA3
Synaptogenesis
BDNF

ABSTRACT

We investigated the effect of β-estradiol (E2) on synaptogenesis in the hippocampus using organotypic hippocampal slice cultures and subregional hippocampal neuron cultures. E2 increased the expression of PSD95, a postsynaptic marker, specifically in stratum lucidum of Cornu Ammonis 3 (CA3SL) in cultured hippocampal slices. E2 also increased the spine density at the proximal site of CA3 apical dendrites in CA3SL and PSD95 was clustered on these spine heads. The effects of E2 on the expression of PSD95 and the spine density disappeared when the dentate gyrus (DG) had been excised at 1 day in vitro (DIV). FM1-43 analysis of subregional hippocampal neuron cultures which were comprised of Ammon's horn neurons, DG neurons, or a mixture of these neurons, revealed that E2 increased the number of presynaptic sites in the cultures that contained DG neurons. K252a, a potent inhibitor of the high affinity receptor of brain-derived neurotrophic factor (BDNF), and function-blocking antibody to BDNF (BDNFAB) completely inhibited the effects of E2 in hippocampal slice cultures and subregional neuron cultures, whereas ICI182,780 (ICI), a strong antagonist of nuclear estrogen receptors (nERs), did not. Expression of BDNF in DG neurons was markedly higher than that in Ammon's horn

* *Corresponding author*. Fax: +81 3 3707 6950.
E-mail address: kasato@nihs.go.jp (K. Sato).

Abbreviations: ACM, astrocyte-conditioned medium; ANOVA, analysis of variance; AraC, cytosine β-D-arabino-furanoside; BDNF, brain-derived neurotrophic factor; BDNFAB, function blocking antibody to BDNF; BSA, bovine serum albumin; CA1, Cornu Ammonis 1; CA3, Cornu Ammonis 3; cAMP, 3′–5′-cyclic adenosine monophosphate; CNS, central nervous system; CREB, PKA/cAMP-responsive element binding protein; DG, dentate gyrus; DIC, differential interference contrast; DiI, 1,1′-dioctadecyl-3,3,3′,3′-tetramethylindocarbocyanine perchlorate; DIV, day(s) in vitro; DMSO, dimethylsufoxide; E2, β-estradiol; ECL, enhanced chemiluminescence; EDTA, ethylenediaminetetraacetic acid; ELISA, enzyme linked immunosorbent assay; ER, estrogen receptor; FM1-43, (*N*-(3-triethylammoniumpropyl)-4-(4-(dibutylamino)styryl)pyridinium dibromide; GABA, γ(gamma)-aminobutyric acid; HBSS, Hank's balanced salt solution; HS, horse serum; ICI, ICI182,780; IgG, immunoglobulin G; LDCVs, large dense-core vesicles; L-Glu, L-glutamate; LTP, long-term-potentiation; MEK, MAP kinase kinase; MEM, minimal essential medium; mER, membrane estrogen receptor; NB, neurobasal medium; nER, nuclear estrogen receptor; NeuN, neuronal nuclear antigen; OD, optical density; P3, postnatal day 3; P8, postnatal day 8; PB, phosphate buffer; PBS, phosphate buffered saline; PDZ, PSD-95-Disks large-zona occludens 1/2; PFA, paraformaldehyde; PKA, cAMP-dependent protein kinase A; PSD95, postsynaptic density protein of 95 kDa; Rp-cAMP, Rp-adenosine 3′, 5′-cyclic monophosphorothioate triethylammonium salt; SDS, sodium dodecyl sulphate; S.E.M., standard error of the mean; SL, stratum lucidum; SO, stratum oliens; SP, stratum pyramidale; SR, stratum radiatum; TBS, Tris-buffered saline; TrkB, the high affinity receptor for several neurotrophins; TTX, tetrodotoxin

0006-8993/$ – see front matter © 2007 Elsevier B.V. All rights reserved.
doi:10.1016/j.brainres.2007.02.093

Please cite this article as: Sato, K., et al., β-Estradiol induces synaptogenesis in the hippocampus by enhancing brain-derived neurotrophic factor release from dentate gyrus granule cells, Brain Res. (2007), doi:10.1016/j.brainres.2007.02.093

UNCORRECTED PROOF

ARTICLE IN PRESS

neurons and E2 did not affect these expression levels. E2 significantly increased the BDNF release from DG neurons. KT5720, a specific inhibitor of 3′–5′-cyclic adenosine monophosphate (cAMP)-dependent protein kinase A (PKA), and Rp-adenosine 3′, 5′-cyclic monophosphorothioate triethylammonium salt (Rp-cAMP), a non-hydrolyzable diastereoisomer and a potent inhibitor of PKA, completely suppressed the E2-induced increase in BDNF release, whereas ICI and U0126, a potent inhibitor of MAP kinase kinase (MEK), did not. These results suggest that E2 induces synaptogenesis between mossy fibers and CA3 neurons by enhancing BDNF release from DG granule cells in a nER-independent and PKA-dependent manner.

© 2007 Elsevier B.V. All rights reserved.

1. Introduction

Estrogens have diverse effects on structure and function of the central nervous system (CNS) (for review, McEwen et al., 2001; Scharfman and MacLusky, 2005; Segal and Murphy, 2001). These effects include enhancement of glutamate-mediated transmission (Woolley, 1998), decreased afterhyperpolarization (Kramar et al., 2004), facilitation of memory (Tyler et al., 2002), increased dendritic spine and spine synapse numbers (Segal and Murphy, 2001), promotion of DG neurogenesis (Tanapat et al., 1999), and increased seizure susceptibility (Woolley and Schwartzkroin, 1998). Such diversity arises because estrogens have multiple mechanisms of action. They modulate gene transcription by interacting with 2 types of nERs, ERα and ERβ. In addition, recent reports clarified nongenomic mechanisms that act via receptors associated

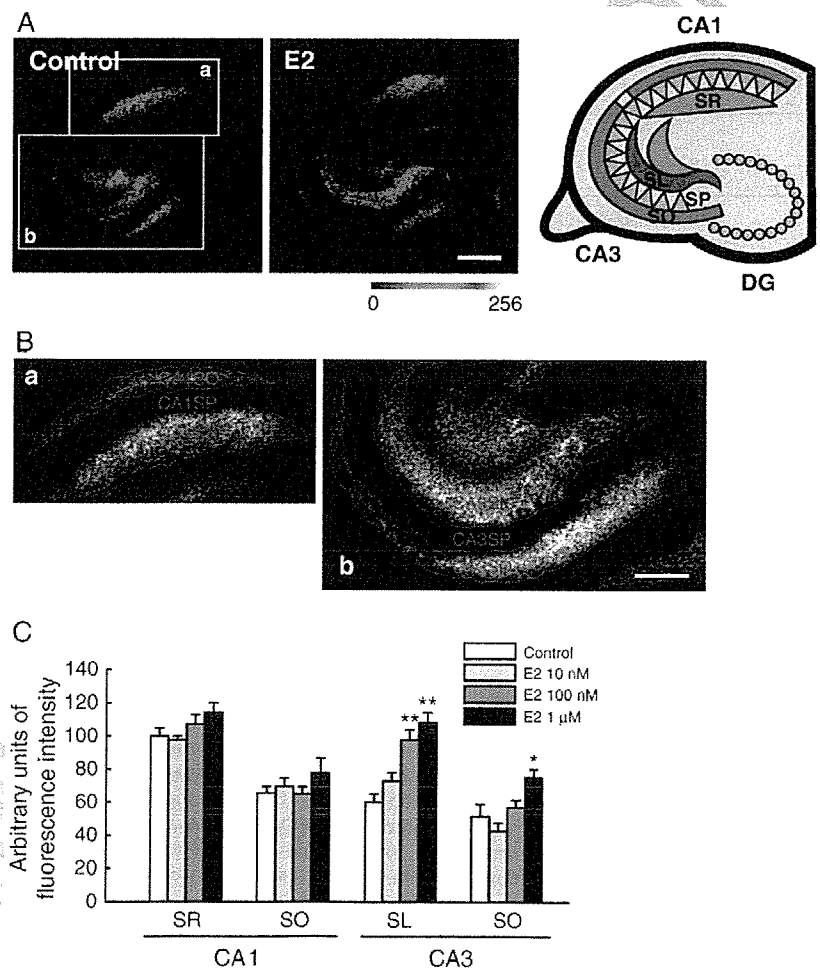

Fig. 1 – Effects of E2 on the expression of PSD95 in cultured hippocampal slices. (A) PSD95 immunoreactive signals in the control slice (left) and the slice treated with E2 (1 μM, 24 h) (middle). Bar=500 μm. (B) Magnified gray-scale images of a and b in A. CA1SR, CA1SO, CA3SL, and CA3SO appeared as fluorescent compartments. Bar=250 μm. (C) Effects of E2 (10 nM–1 μM, 24 h) on the expression of PSD95. E2 increased the expression level of PSD95 dose-dependently in CA3SL. *: $p<0.05$, **: $p<0.01$ vs. the control group in each region. $N=8$, Tukey's test following ANOVA.

Please cite this article as: Sato, K., et al., β-Estradiol induces synaptogenesis in the hippocampus by enhancing brain-derived neurotrophic factor release from dentate gyrus granule cells, Brain Res. (2007), doi:10.1016/j.brainres.2007.02.093

with or integral to plasma membrane (mERs), thereby activating signaling cascades distinct from those of nERs (Beyer et al., 2003; Kelly and Levin, 2001; Segars and Driggers, 2002). We previously reported that pretreatment with estrogens increased neuronal sensitivity to L-glutamate (L-glu) specifically in CA3 in organotypic hippocampal slice cultures. In the same study we found that these effects were mediated by the mechanisms that did not involve nERs (Sato et al., 2002). These results raised the possibility that estrogens affect synaptic contacts in CA3. In the present study, we therefore investigated the effects of E2 on synaptogenesis in the hippocampus and explored the underlying mechanisms using 2 experimental systems. Firstly, we investigated the effects of E2 on the expression of PSD95, a postsynaptic marker, and the spine density in cultured hippocampal slices. Secondly, we investigated the effects of E2 on the number of presynaptic release sites in subregional hippocampal neuron cultures, which were comprised of Ammon's horn neurons, DG neurons, or a mixture of these neurons. It has been reported that in the hippocampus the highest concentration of BDNF occurs in DG granule cells, especially in their axons, mossy fibers (Dieni and Rees, 2002; Scharfman et al., 2003), from the prenatal period through to adulthood (Dieni and Rees, 2002). Although BDNF is known to promote synaptogenesis (Aguado et al., 2003; Alsina et al., 2001; Seil and Drake-Baumann, 2000), it has not been elucidated whether the BDNF in DG granule cells has a role in hippocampal synapse formation. For this reason, we also investigated the relationship between endogenous BDNF in DG granule cells and the effects of E2 in CA3. We here provide evidence showing that E2 induces synaptogenesis between mossy fibers and CA3 neurons by enhancing BDNF release from DG granule cells in a nER-independent and PKA-dependent manner.

2. Results

2.1. *Effects of E2 on postsynaptic sites in cultured hippocampal slices*

We first examined the effect of E2 on the expression of PSD95 in cultured hippocampal slices immunohistochemically. PSD95 is one of the PDZ (PSD-95-Disks large-zona occludens 1/2) domain-containing proteins (Craven and Bredt, 1998; Garner et al., 2000) and is an integral protein of the postsynaptic density. In the control group, the fluorescent signals for PSD95 were apparent in the major hippocampal synaptic sites, i.e., stratum radiatum (SR), stratum oriens (SO), SL and the dentate hilar region (Fig. 1A, left). Because in this study slices were cultured after removing entorhinal cortex, we quantified the expression of PSD95 in CA1SR, CA1SO, CA3SL, and CA3SO, the synaptic sires which maintain the intact presynaptic and postsynaptic cells. CA1SR, CA1SO, CA3SL, and CA3SO appeared as fluorescent compartments (Figs. 1B, a and b) in magnified gray-scale mode images, we regarded the averaged fluorescence intensity of each compartment (an outlined area) as the expression level of PSD95 of each synaptic site (see Experimental procedures). When we compared the effects of E2 on the PSD95 expression in CA1 and CA3, E2 (24 h) increased the expression of PSD95 dose-dependently in CA3SL and the effects were significant at 100 nM and the higher concentration (Figs. 1A middle and B). Although E2 also increased the PSD 95 expression in CA3SO at 1 μM (145±9.75% of control), the effect was weaker than that in CA3SL (180±10.2% of control at 1 μM). The distribution pattern of PSD95 signals (including area) in each region was not affected by E2. We then investigated the effect of E2 on the spine density in CA3SL using 1,1′-dioctadecyl-3,3,3′,3′-tetramethylindocarbocyanine perchlorate (DiI) staining. E2 (1 μM, 24 h) markedly increased the spine density at the proximal site of CA3 apical dendrites in CA3SL (296±24.3% of control; Figs. 2A and B). E2 also increased the spine density at the proximal site of CA1 apical dendrites in CA1SR (132±4.49% of control), although to a much lesser extent than that in CA3SL (Fig. 2A). Fig. 2B shows typical images of the proximal sites of CA3 apical dendrites in the control slice (left) and in the E2-treated slice (right). When we immunostained the E2-treated slices with anti-PSD95 antibody after DiI staining, most PSD95 signals in CA3SL clustered on the spine heads (Fig. 2A, right). These results indicate that E2 increased the number of postsynaptic sites in CA3SL. CA3SL is the region in which mossy fibers (DG granule cell axons) make synapses with CA3 pyramidal neurons. We then investigated the effect of E2 on the expression of PSD95 and the spine density in CA3 in DG (–) slices, i.e., the slices of which DG had been excised at 1 DIV. As shown by

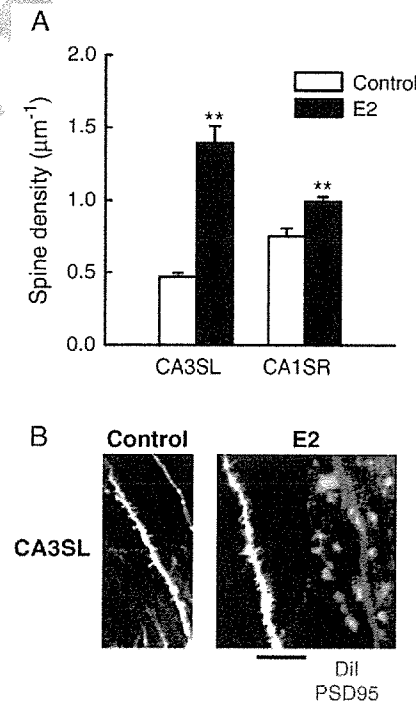

Fig. 2 – Effects of E2 on the spine density in cultured hippocampal slices. (A) E2 (1 μM, 24 h) markedly increased the spine density in CA3SL. **: $p<0.01$ vs. the vehicle control group in each region. $N=8$, Student's t test. (B) Typical images of the DiI-labeled CA3 apical dendrites in the control slice (left) and the E2-treated slice (right). Double staining with DiI and anti-PSD95 antibody revealed that in the E2-treated slice most PSD95 signals (green) were clustered on the spine-heads of the CA3 apical dendrites (red). Bar=5 μm.

UNCORRECTED PROOF

Please cite this article as: Sato, K., et al., β-Estradiol induces synaptogenesis in the hippocampus by enhancing brain-derived neurotrophic factor release from dentate gyrus granule cells, Brain Res. (2007), doi:10.1016/j.brainres.2007.02.093

Nissl staining, the viability of CA3 pyramidal neurons was not altered by the dissection of the DG (Fig. 3A). The distribution pattern of the PSD95 signals was not affected, either (Fig. 3B). E2 (1 μM, 24 h) affected neither the expression level (Fig. 3C) nor the distribution pattern of PSD95 in DG (–) slices (data not shown). The effect of E2 (1 μM, 24 h) on the spine density in CA3SL was also abolished in DG (–) slices (Fig. 3D). Taken together, these results suggest that E2 induces synaptogenesis between mossy fibers and CA3 pyramidal neurons.

2.2. *Effects of E2 on presynaptic sites in subregional hippocampal neuron cultures*

We next investigated the effect of E2 on the number of presynaptic sites using subregional hippocampal neuron cultures, which were comprised of Ammon's horn neurons, DG neurons, or a mixture of these neurons, respectively. We quantified the number of presynaptic sites by counting the number of sites in which depolarization-induced uptake and release of (*N*-(3-triethylammoniumpropyl)-4-(4-(dibutylamino)styryl)pyridinium dibromide (FM1-43) (Cochilla et al., 1999) had occurred (see Experimental procedures). Fig. 4A shows the typical morphologies of neurons in the Ammon's horn neuron culture (left) and in the DG neuron culture (middle). Most cells in the Ammon's horn neuron culture were large and spindle-shaped, whereas most cells in the DG neuron culture were small and granular. As shown in Fig. 4B, E2 (1 μM, 24 h) significantly increased the number of presynaptic sites in the mixed neuron culture (199±9.18% of control). E2 also increased the number of presynaptic sites in the DG neuron culture (170±12.1% of control), but not in the Ammon's horn neuron culture. Fig. 4C shows the typical fluorescent images of presynaptic sites (red puncta) in the control group (top left) and in the E2-treated group (top right) in the mixed neuron culture. We confirmed that E2 had no effect on the number of surviving neurons in each culture by immunostaining with anti-NeuN antibody (data not shown). These results indicate that E2 increased the number of presynaptic sites in the hippocampal neuron cultures and that DG neurons are indispensable for this effect.

2.3. *The effects of E2 in hippocampal slice cultures and subregional hippocampal neuron cultures were mediated by the mechanism which is independent of nERs and dependent on endogenous BDNF*

Pharmacological experiments were performed to investigate and compare the mechanisms underlying the effects of E2 in hippocampal slice cultures and subregional hippocampal neuron cultures (the mixed neuron culture) (Fig. 5). First, we examined the contribution of nERs using ICI, a strong antagonist to both of ERα (Ki: 1.5 nM) and ERβ (Ki: 6.4 nM) (Kuiper et al., 1997). ICI at a concentration of 1 μM did not alter the effect of E2 on the expression of PSD95 expression, the spine density, and the number of presynaptic sites (Figs. 5A–C). It has been reported that DG granule cells have the highest concentration of BDNF in the hippocampus, especially in the mossy fibers (Dieni and Rees, 2002; Scharfman et al., 2003). Because BDNF is known to enhance synapse formation (Aguado et al., 2003; Alsina et al., 2001; Seil and Drake-

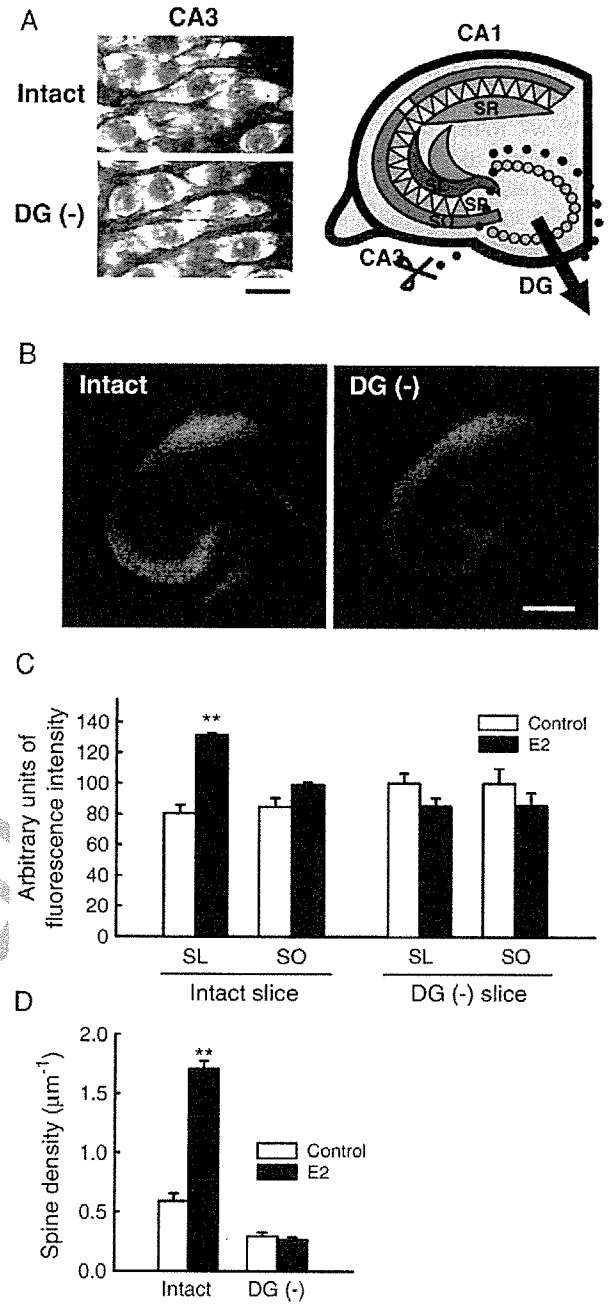

Fig. 3 – Effects of E2 on the expression of PSD95 and the spine density in cultured hippocampal slices of which DG had been excised at 1 DIV. (A) The viability of CA3 pyramidal neurons in DG (–) slices. Nissl staining revealed that their viability was not affected by the dissection of DG. Bar=20 μm. (B) Immunoreactive signals of PSD95 in a DG (–) slice. The distribution pattern of the PSD95 signals was not affected by the dissection of DG. Bar=500 μm. (C) The effect of E2 on the expression of PSD95 in DG (–) slices. E2 (1 μM, 24 h) did not affect the expression of PSD95 in CA3 in DG (–) slices. (D) The effect of E2 on the spine density in CA3SL in DG (–) slices. E2 (1 μM, 24 h) did not affect the spine density in CA3SL in DG (–) slices.

UNCORRECTED

Please cite this article as: Sato, K., et al., β-Estradiol induces synaptogenesis in the hippocampus by enhancing brain-derived neurotrophic factor release from dentate gyrus granule cells, Brain Res. (2007), doi:10.1016/j.brainres.2007.02.093

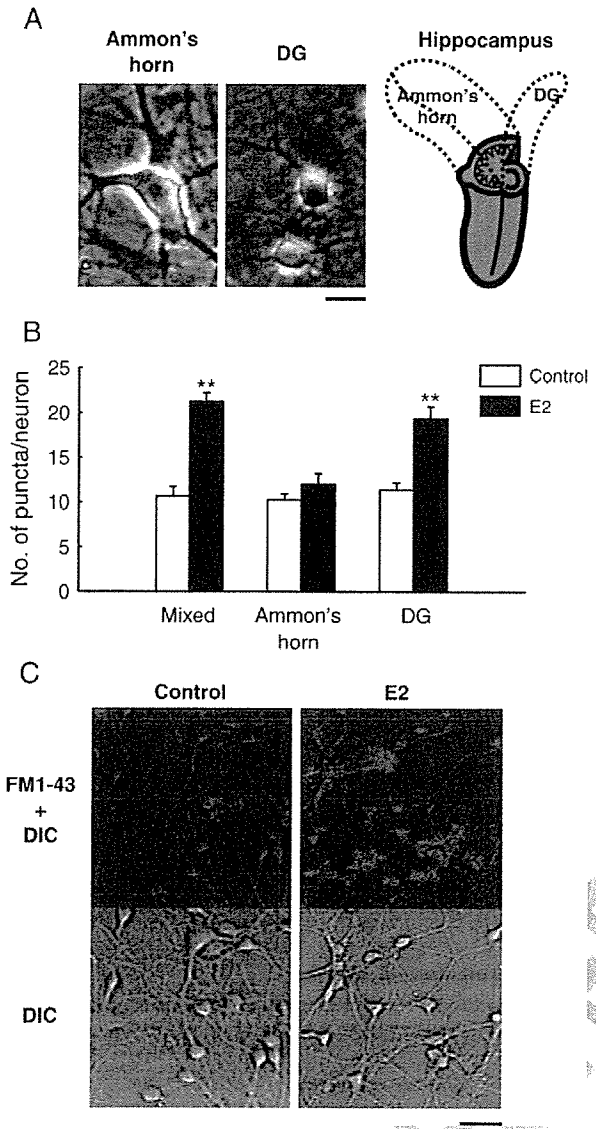

Fig. 4 – Effects of E2 on the number of presynaptic sites in subregional hippocampal neuron cultures. (A) Typical cell morphologies in the Ammon's horn neuron culture (left) and in the DG neuron culture (middle). Bar=20 μm. (B) E2 (1 μM, 24 h) significantly increased the number of presynaptic sites in the mixed neuron culture and in the DG neuron culture. **: $p<0.01$ vs. the control group in each culture. $N=8$, Student's t test. (C) Typical images of presynaptic sites visualized by FM1-43 (red puncta) in the control group (top left) and in the E2-treated group (top right) in the mixed neuron culture. DIC images of the same microscopic views were also shown (bottom left and bottom right). Bar=50 μm.

205 Baumann, 2000), we examined the involvement of BDNF in the
206 effects of E2. K252a (200 nM), a potent inhibitor of the high
207 affinity receptor of BDNF (TrkB) (Squinto et al., 1991; Bothwell,
208 1995), significantly inhibited the effects of E2 on the expres-
209 sion of PSD95 expression, the spine density, and the number of
210 presynaptic sites (Figs. 5A–C). Furthermore BDNFAB (10 μg/ml)
211 significantly inhibited the effects of E2 in these experiments
212 (Figs. 5A–C). These inhibitors alone had no effects in each case.
213 These results indicate that the effects of E2 in hippocampal

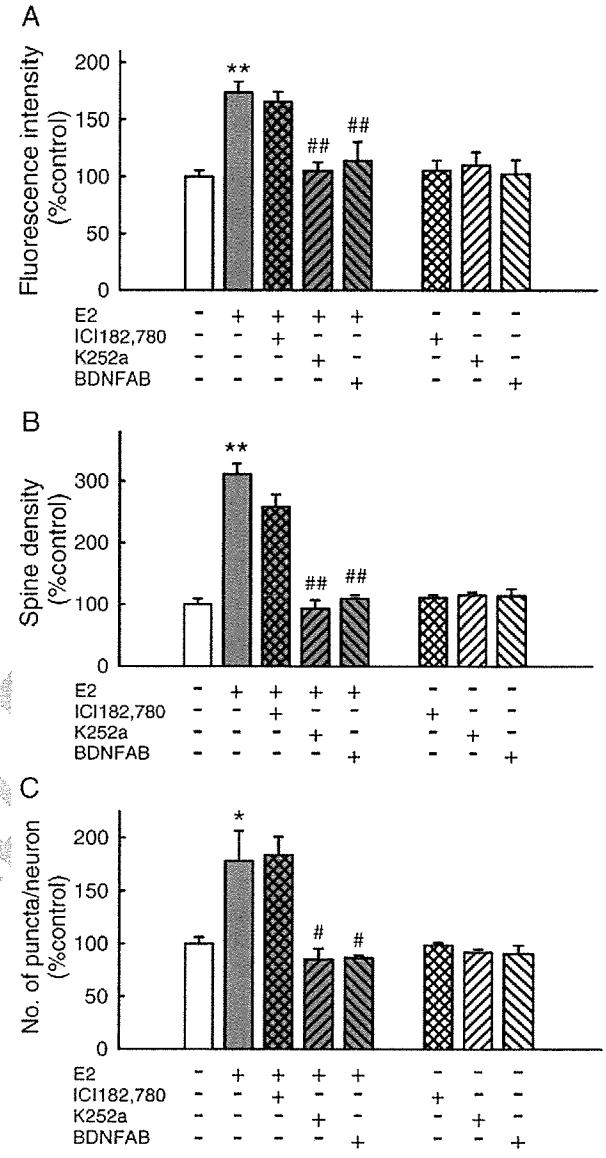

Fig. 5 – Effects of ICI, K252a, and BDNFAB on the effects of E2 in hippocampal slice cultures and subregional hippocampal neuron cultures. (A) K252a (200 nM) and BDNFAB (10 μg/ml) significantly inhibited the effect of E2 on the expression of PSD95 in cultured hippocampal slices, whereas ICI (1 μM) did not. **: $p<0.01$ vs. the control group, ##: $p<0.01$ vs. the E2-treated group. $N=8$, Tukey's test following ANOVA. (B) K252a (200 nM) and BDNFAB (10 μg/ml) significantly inhibited the effect of E2 on the spine density in cultured hippocampal slices, whereas ICI (1 μM) did not. **: $p<0.01$ vs. the control group, ##: $p<0.01$ vs. the E2-treated group. $N=8$, Tukey's test following ANOVA. (C) K252a (200 nM) and BDNFAB (10 μg/ml) significantly inhibited the effect of E2 on the number of presynaptic sites in the mixed neuron culture, whereas ICI (1 μM) did not. *: $p<0.05$ vs. the control group, #: $p<0.05$ vs. the E2-treated group. $N=8$, Tukey's test following ANOVA.

Please cite this article as: Sato, K., et al., β-Estradiol induces synaptogenesis in the hippocampus by enhancing brain-derived neurotrophic factor release from dentate gyrus granule cells, Brain Res. (2007), doi:10.1016/j.brainres.2007.02.093

slice cultures and subregional neuron cultures were mediated by the common mechanism which is independent of nERs and dependent on endogenous BDNF, suggesting the involvement of BDNF in DG granule cells in the synaptogenic effect of E2 in CA3SL.

2.4. *E2 enhanced BDNF release from DG granule cells via nER-independent and PKA-dependent mechanisms*

We further examined the association between the effects of E2 and BDNF using subregional hippocampal neuron cultures. The expression levels of BDNF were confirmed for both the Ammon's horn neuron culture and the DG neuron culture by Western blot analysis and enzyme linked immunosorbent assay (ELISA) (Fig. 6). In Western blot analysis, BDNF immunoreactive bands were detected in the control lanes for both cultures, but the OD for the DG neurons was markedly higher than that for the Ammon's horn neurons (Fig. 6A). E2 (1 μM, 24 h) did not affect the expression levels of BNDF in Ammon's horn neurons or DG neurons. ELISA also showed that the expression level of BDNF in DG neurons was remarkably higher than that of Ammon's horn neurons and E2 had no effect on the expression levels in both cultures (Fig. 6B). These results indicate that subregional neuron cultures reflect in vivo pattern of BDNF expression in the hippocampus, in which the highest concentration of BDNF occurs in DG granule cells (Dieni and Rees, 2002; Scharfman et al., 2003). We next examined the possibility that E2 enhances BDNF release from DG granule cells without affecting BDNF expression. The amount of BDNF released into the culture medium of the DG neuron culture was measured by ELISA. We performed ELISA after 10 h of treatment with E2, at the time point when the effect of E2 on the number of presynaptic sites was not yet apparent (Fig. 7A). E2 (1 μM, 10 h) remarkably increased the BDNF release (267 ± 20.5% of control; Fig. 7B). Neither ICI (1 μM) nor U0126 (10 μM) (Ki: 72 nM for MEK1, 58 nM for MEK2) (Duncia et al., 1998), influenced the effect of E2. In contrast, KT5720 (200 nM) (Ki: 56 nM for PKA) (Kase et al., 1987) and Rp-cAMP (10 μM) (Ki: 11 μM for PKA) (Rothermel and Parker Botelho, 1988), suppressed the effect of E2 to the control level. These inhibitors alone had no effects on the basal BDNF release. These results indicate that E2 enhanced BDNF release from DG

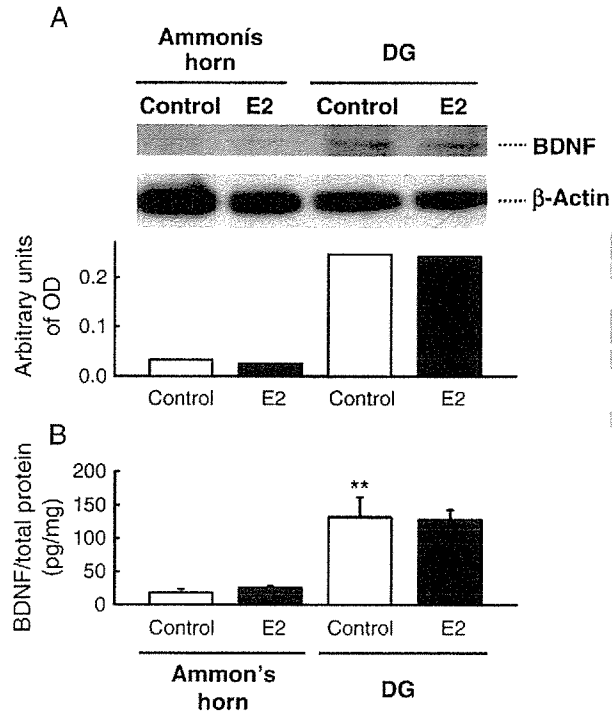

Fig. 6 – The expression of BDNF in subregional hippocampal neuron cultures. (A) Western blot analysis of BDNF in subregional hippocampal neuron cultures. The expression level of BDNF of DG neurons was much higher than that of Ammon's horn neurons. E2 (1 μM, 24 h) had no effect on the BDNF expression level. The same results were obtained in 3 independent experiments. (B) ELISA detection of BDNF in subregional hippocampal neuron cultures. The expression level of BDNF in DG neurons was significantly higher than that in Ammon's horn neurons. E2 (1 μM, 24 h) had no effect on the BDNF expression level. **: $p<0.01$ vs. the control group of Ammon's horn neurons. $N=4$, Tukey's test following ANOVA.

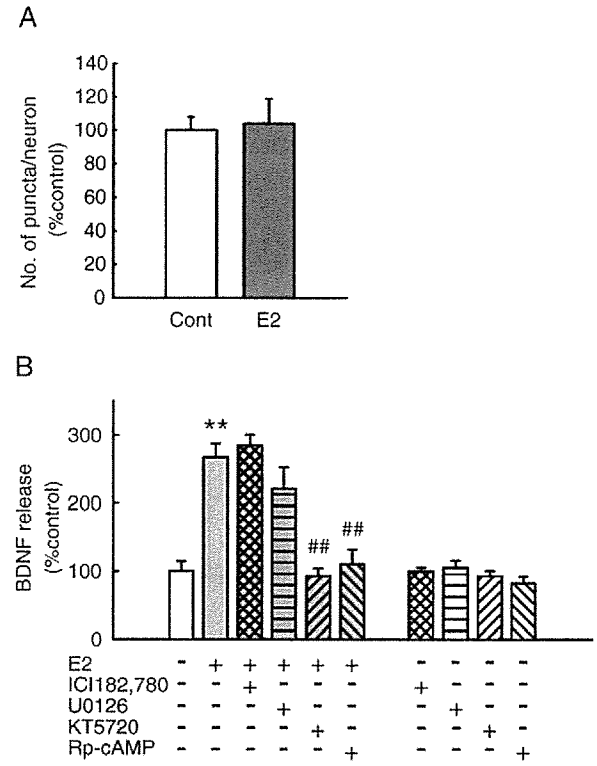

Fig. 7 – Effects of E2 on the BDNF release in the DG neuron culture. (A) Treatment for 10 h with E2 (1 μM) had no effect on the number of presynaptic sites in the DG neuron culture. (B) E2 (1 μM, 10 h) significantly enhanced BDNF release in the DG neuron culture. KT5720 (200 nM) and Rp-cAMP (10 μM) inhibited the effect of E2, whereas ICI (1 μM) and U0126 (10 μM) did not. **: $p<0.01$ vs. the control group, ##: $p<0.01$ vs. the E2-treated group. $N=4$, Tukey's test following ANOVA.

Please cite this article as: Sato, K., et al., β-Estradiol induces synaptogenesis in the hippocampus by enhancing brain-derived neurotrophic factor release from dentate gyrus granule cells, Brain Res. (2007), doi:10.1016/j.brainres.2007.02.093

granule cells via nER-independent and PKA-dependent mechanisms, which may underlie the effects of E2 described above.

3. Discussion

In this study, we provided evidence showing that E2 induces synaptogenesis between mossy fibers and CA3 neurons by enhancing BDNF release from DG granule cells in a nER-independent and PKA-dependent manner.

We used subregional hippocampal neuron cultures to investigate the effects of E2 in detail. That these cultures sufficiently maintain their region-specific characters is supported by the following evidence: 1) the morphology of neurons in the Ammon's horn neuron culture was clearly different from that in the DG neuron culture (Fig. 4A). Most cells in the Ammon's horn neuron culture were large and spindle-shaped, which is typical for pyramidal neurons. Most cells in the DG neuron culture were small and granular, which is typical for DG granule cells. 2) DG neurons isolated and cultured using a similar procedure maintain their in vivo physiological properties (Ikegaya et al., 2000). 3) The expression level of BDNF of the cultured DG neurons is much higher than that of the cultured Ammon's horn neurons, reflecting in vivo pattern of BDNF expression in the hippocampus, in which the highest concentration of BDNF occurs in DG granule cells (Dieni and Rees, 2002; Scharfman et al., 2003).

In our study, we prepared hippocampal slices from both genders of P8 rat pups and cultured for 10 days with medium supplemented with horse serum (HS) collected from gelding horses, in which steroid concentrations were under the limits for detection. Because the increases in the expression level of PSD95 and the spine density in CA3 were observed in all slices treated with E2, we consider that the effects of E2 in our study are gender-independent. Currently we are investigating whether or not there is gender difference in the extents of the effects of E2. Organotypic hippocampal slice cultures of P5–9 rat brains are well-established, stable model for investigating hippocampal function including developmental synaptogenesis because neurons maintain synaptogenic ability in each region (CA1, CA3, and DG) (De Simoni et al., 2003; Mizuhashi et al., 2001; Qin et al., 2001). It has been reported that during postnatal development, the capacity of estrogen binding protein is high enough to lower the concentrations of serum estrogens to nonphysiological levels (Germain et al., 1978). This suggests that the conditions for the hippocampal slice culture in the present study more closely represent the postnatal developmental stage. Recently it was clarified that E2 is synthesized from endogenous cholesterol by P45017α and P450 aromatase in hippocampal neurons (Hojo et al., 2004) and that it plays an essential role in the maintenance of synapses (Kretz et al., 2004). The effects of E2 shown here might be achieved by locally synthesized E2 at the postnatal developmental stage. Two previous studies reported the effects of E2 on spinogenesis in cultured hippocampal slices (Kretz et al., 2004; Pozzo-Miller et al., 1999), but their results are conflicting, perhaps because of the effects of various steroids included in the HS in the culture medium.

Our findings suggest that BDNF in DG granule cells mediates the effects of E2. It has been reported that in the hippocampus the highest concentration of BDNF occurs in DG granule cells, especially in their axons, mossy fibers (Dieni and Rees, 2002; Scharfman et al., 2003), from the prenatal period through to adulthood (Dieni and Rees, 2002). The significance of BDNF in DG granule cells, however, had been unknown until Scharfman et al. showed that endogenous BDNF in mossy fibers affected the excitability of CA3 neurons in adult female rats (Scharfman et al., 2003). On the other hand, BDNF has long been known to promote synaptogenesis by maturation of presynaptic sites (Aguado et al., 2003; Seil and Drake-Baumann, 2000). Real-time monitoring revealed that BDNF increases the number of presynaptic sites (Alsina et al., 2001). Presynaptic maturation can induce postsynaptic maturation, as shown by mossy fiber induction of postsynaptic maturation including assembly and clustering of PSD95 on CA3 apical dendrites (Qin et al., 2001). In the present study, BDNF released from DG granule cells may have first increased the number of presynaptic sites by autocrine/paracrine mechanisms, thereby inducing the maturation of postsynaptic sites. In addition to the communication with CA3 pyramidal neurons through giant boutons, mossy fibers also communicate with local circuit interneurons in CA3 through filopodial extensions and en passant boutons (Acsady et al., 1998; Lawrence and McBain, 2003). Although the number of these small terminals is greater than that of giant boutons, we consider that E2 predominantly promoted the synaptogenesis between mossy fibers and CA3 pyramidal neurons in this study because of the following reasons: 1) E2 increased the number of giant boutons, which were identified as mossy fiber terminals containing Zn^{2+} in our previous report (Sato et al., 2002), and 2) the major population of BDNF-positive mossy fiber terminals is those with giant boutons (Danzer and McNamara, 2004). Further experiments using interneuron-specific markers will be necessary to identify the effect of E2 on synaptogenesis between mossy fibers and CA3 interneurons.

E2 enhanced BDNF release from DG granule cells in a nER-independent and PKA-dependent manner. Besides the genomic effects via nERs (ERα and ERβ), recent reports have described the nongenomic effects of estrogens mediated by mERs (Beyer et al., 2003; Kelly and Levin, 2001; Segars and Driggers, 2002). Although the membrane localization of the E2 binding sites is widely accepted, mERs still await isolation and gene cloning. One of the candidate mERs is membrane-localized ERα/β that can activate signal transduction pathways distinct from nERα/β (Razandi et al., 2004; Thomas et al., 2004). Although the mode of action has not been elucidated precisely, ERα has been localized to the neuronal plasma membrane in the hippocampus (Clarke et al., 2000). On the other hand, several reports suggest that the proteins, which are completely different from ERα/β, function as mERs in hypothalamus (Cambiasso and Carrer, 2001), midbrain (Beyer and Karolczak, 2000; Beyer et al., 2002), and neocortex (Toran-Allerand et al., 2002). The effects of E2 observed in our study may have been mediated by one or more mechanisms other than nERs.

It has been reported that E2 modulates the expression of BDNF by genomic (Sohrabji et al., 1995) or nongenomic mechanisms (Ivanova et al., 2001). Unexpectedly, in this

Please cite this article as: Sato, K., et al., β-Estradiol induces synaptogenesis in the hippocampus by enhancing brain-derived neurotrophic factor release from dentate gyrus granule cells, Brain Res. (2007), doi:10.1016/j.brainres.2007.02.093

study BDNF expression levels were not affected by E2 (Fig. 6). Instead, E2 enhanced BDNF release from DG granule cells via the activation of the PKA pathway. The PKA/cAMP-responsive element binding protein (CREB) pathway has been shown to lie downstream of mERs in midbrain dopamine neurons (Beyer and Karolczak, 2000; Beyer et al., 2002). The effects of E2 in this study might be mediated by the same type of mERs as those in midbrain dopamine neurons. There are 2 major BDNF secretory pathways (for review, Lessmann et al., 2003): one is the Ca^{2+}-independent constitutive pathway and the other is the Ca^{2+}-dependent regulated pathway. In the regulated pathway, BDNF is sorted to large dense-core vesicles (LDCVs) (Wu et al., 2004) and released in an activity-dependent manner (Haubensak et al., 1998) following slow kinetics typical for protein secretion (Hartmann et al., 2001). BDNF plays an important role in long-term synaptic plasticity (for review, McAllister et al., 1999). BDNF is released selectively by electrical stimulation patterns that induce long-term-potentiation (LTP), thereby modulating the activity-dependent neuronal plasticity (Balkowiec and Katz, 2002; Gartner and Staiger, 2002). cAMP triggers BDNF release in such LTP-inducing condition (Patterson et al., 2001), so E2 might affect synaptic plasticity by way of cAMP-dependent BDNF release.

In ovariectomized adult female rats, E2 enhances the spinogenesis of apical dendrites in CA1 but not in CA3 (Gould et al., 1990). Recent studies have revealed that Akt (protein kinase B) activation via mERs mediates the spinogenesis in CA1 in adult rats (McEwen et al., 2001; Znamensky et al., 2003). On the other hand, there is evidence for another mechanism of E2-induced spinogenesis in embryonic hippocampal neuron cultures. In this system E2 acts via nERs to suppress BDNF expression in γ(gamma)-aminobutyric acid (GABA) ergic interneurons and to decrease GABAergic inhibition, thereby inducing spinogenesis (Murphy et al., 1998a; Murphy et al., 1998b). It is possible that these mechanisms were also active in our study because E2 increased the spine density in CA1SR in cultured hippocampal slices. But clear differences were observed between the effect in CA1SR and that in CA3SL. The spinogenic effect in CA1SR was much weaker than that in CA3SL (Fig. 2) and the expression of PSD95 in CA1SR was not changed by E2 (Fig. 1). The local assembly of PSD95 is spatially and temporally correlated with the maturation of spine morphogenesis (Okabe et al., 2001: Jontes and Smith, 2000). PSD95 clusters are found in one-half of dendritic filopodia, but in most mature spines (Takahashi et al., 2003). Thus, the spines induced by E2 in CA1SR may be more immature compared with those in CA3SL. The effects of E2 in CA3 through BDNF derived from DG granule cells may be stronger than that in CA1 through the mechanisms described above. The absence of the effect of E2 in CA3 in previous reports (Gould et al., 1990; Znamensky et al., 2003) can be explained if the mechanism that we indicated here is not active in adulthood or the mechanisms demonstrated in the previous reports are active predominantly in CA1.

Our results strongly suggest that E2 induces synaptogenesis between mossy fibers and CA3 neurons by the enhancement of BDNF release from DG granule cells in a nER-independent and PKA-dependent manner. These data provide evidence that BDNF in DG granule cells has a role in synaptogenesis, and that E2 can modulate this synaptogenic function of BDNF.

4. Experimental procedure

4.1. *Materials*

Millicell-CM was from Millipore (Bedford, MA). Minimal essential medium (MEM), Neurobasal medium (NB) and B-27 supplement were from Gibco Invitrogen Co. (Carlsbad, CA). Donor HS (gelding) was from C-C Biotech Corporation (Valley Center, CA). Paraformaldehyde (PFA), polyoxyethylene (10) octylphenyl ether (Triton X-100), ammonium chloride, dimethylsufoxide (DMSO), L-glutamine, glycine, Tween 20 and sodium azide were from Wako Pure Chemical (Osaka, Japan). K252a was from Calbiochem (Darmstadt, Germany). Anti-BDNF antibodies (AB1534SP and AB1513P) and Chemikine BDNF Sandwich ELISA kit were from Chemicon (Temecula, CA). ICI was from Tocris (Ballwin, MO). Mouse monoclonal immunoglobulin G (IgG) to PSD95 (K28/43) was from Upstate Biotechnology (Lake Placid, NY). Alexa Fluor 488 rabbit anti-mouse IgG, NeuroTrace fluorescent Nissl, DiI and FM1-43 were from Molecular Probes (Eugene, OR). E2, poly-L-lysine, cytosine β-D-arabino-furanoside (AraC), ethylenediaminetetraacetic acid (EDTA), phenylmethylsulphonyl fluoride, leupeptin, antipain hydrochloride, aprotinin, Trizma hydrochloride, bovine serum albumin (BSA), rabbit polyclonal IgG to β-actin, peroxidase-conjugated anti-rabbit IgG, tetrodotoxin (TTX), KT5720, and Rp-cAMP were from Sigma (St. Louis, MO). U0126 was from Promega (Madison, WI). Sodium dodecyl sulphate (SDS) was from Nacalai tesque (Kyoto, Japan). ADVASEP-7 was from Biotium (Hayward, CA). Enhanced chemiluminescence (ECL) plus Western blotting detection kit was from Amersham Biosciences (Arlington Heights, IL). Fluorescent images were obtained using a BioRad μ-Radiance laser scanning confocal system (Hercules, CA) attached to Nikon inverted microscope (Tokyo, Japan). Image analysis was performed using Adobe Photoshop 7.0 (Mountain View, CA).

4.2. *Organotypic hippocampal slice culture*

All animal procedures were in accordance with the guidelines of the National Institute of Health Sciences, Japan, to minimize pain or discomfort. Organotypic slice cultures of both genders of P8 Wistar rat hippocampi were prepared according to the method of Sato et al. (2002). Briefly, horizontal medial hippocampal slices (300-μm thick) were placed on Millicell-CM transmembranes and cultured with 0.7 ml of the culture media (50% [vol/vol] MEM, 25% [vol/vol] Hank's balanced salt solution [HBSS], and 25% [vol/vol] HS [gelding] supplemented with 6.5 mg/ml glucose, 50 U/ml penicillin G potassium and 100 μg/ml streptomycinsulphate). All experiments were performed at 10 days in vitro (DIV) because cultured hippocampal slices recover from damage by sectioning and complete the trisynaptic neuronal circuitry (DG→CA3→CA1) at 10–14 DIV (Nakagami et al., 1997).

Please cite this article as: Sato, K., et al., β-Estradiol induces synaptogenesis in the hippocampus by enhancing brain-derived neurotrophic factor release from dentate gyrus granule cells, Brain Res. (2007), doi:10.1016/j.brainres.2007.02.093

4.3. *Immunohistochemistry*

Immunostaining of cultured hippocampal slices was performed according to the method of Qin et al. (2001) with modifications. Slices were fixed with ice-cold 4% (wt/vol) PFA in 0.1 M phosphate buffer (PB) for 10 min at 4 °C, washed with phosphate buffered saline (PBS) (5 min×3), and treated with 1% (vol/vol) Triton X-100 in PBS overnight at 4 °C. Slices were then blocked with 50 mM ammonium chloride for 30 min at 4 °C and 20% HS in PBS for 30 min at 4 °C. Subsequent steps were carried out using PBS containing 1% HS. Slices were treated with mouse monoclonal IgG to PSD95 (1:1000) overnight at 4 °C, washed (15 min×3), and treated with Alexa Fluor 488 rabbit anti-mouse IgG (1:1000) overnight at 4 °C. After washing (15 min×3), fluorescent images were obtained by confocal microscopy (BioRad μ-Radiance laser scanning confocal system) using a 4×objective. Black level was set so that the averaged fluorescence intensity of 5 independent squares (20 μm×20 μm) placed at the medial position of CA1 stratum pyramidale (SP) of the control slice had the same value as that of the outside of the slice. Gain level was set so that the averaged fluorescence intensity of 5 squares (20 μm×20 μm) placed at the medial position of CA3SL of the control slice was at the half-maximum level. In gray-scale mode under these settings, the major synaptic sites appeared as fluorescent compartments as shown in Fig. 1B. When we outlined these compartments as indicated in Fig. 1B and calculated the areas, the values were constant regardless of the treatment (data not shown), so, we measured the averaged fluorescence intensity of each compartment (an outlined area) and subtracted the back ground intensity to quantify the expression level of PSD95 of each synaptic site. Because slices were cultured after removing entorhinal cortex, we quantified the expression of PSD95 in CA1SR, CA1SO, CA3SL, and CA3SO, the synaptic sites which maintain the intact presynaptic and postsynaptic cells (Fig. 1B).

4.4. *DiI staining*

Cultured hippocampal slices were fixed with 4% PFA for 30 min at 4 °C. The fixative above the transmembrane was removed and DiI crystals were embedded into CA1SO and CA3SO under the light microscope. After 3 days of incubation at 4 °C, fluorescent images were obtained by confocal microscopy using a 60×objective. Horizontal optical sections were taken at 0.5 μm steps and the resultant z-series images were summed into a flat image. Spines (both dendritic filopodia and mature spines) were counted at the proximal sites of apical dendrites projecting from pyramidal cell bodies. For double labeling with DiI and PSD95 immunostaining, slices were immunostained after 3 days of incubation with DiI crystals.

4.5. *Fluorescent Nissl staining*

Cultured hippocampal slices were fixed with 4% PFA for 60 min at 4 °C. Subsequent steps were carried out at room temperature. After washing with PBS (15 min×3), the slices were treated with 0.1% Triton X-100 in PBS for 60 min, washed with PBS for 10 min, and incubated with NeuroTrace fluorescent Nissl (1:30 in PBS) for 40 min in a dark room. The incubation was terminated by a 10 min wash with 0.1% Triton X-100 in PBS, followed by 2 h wash with PBS. Fluorescent images were obtained by confocal microscopy using a 60×objective.

4.6. *Subregional hippocampal neuron culture*

Subregional neuron cultures of both genders of P3 Wistar rat hippocampi were prepared according to the method of Ikegaya et al. (2000). Ammon's horn and DG were isolated from hippocampi with extreme care so as not to mix these 2 regions (Fig. 4A, right). Dissociated cells from Ammon's horn, DG, or a combination of these regions were suspended in a 1:1 mixture of astrocyte-conditioned medium (ACM) and NB/B27 medium (2% [v/v] B-27 supplement, 73 μg/ml L-glutamine in NB) and plated onto 48-well plates coated with poly-L-lysine. After 24 h, the medium was changed to ACM-free NB/B-27 medium containing 2 μM AraC. Cells derived from each region were cultured for 7 days at the same cell density (2×10^4 cells/cm^2 for FM1-43 analysis, 5×10^5 cells/cm^2 for Western blot analysis and ELISA detection of BDNF). All surviving cells were immunohistochemically confirmed to be neurons using anti-NeuN antibody (data not shown).

4.7. *FM1-43 analysis*

After 1 h of incubation with HBSS at 37 °C, cultured neurons were treated with 10 μM FM1-43, a styryl pyridinium dye (Cochilla et al., 1999) in high K^+-HBSS (20 mM KCl; osmolarity maintained by concomitant decrease in sodium concentration) for 2 min and washed gently with HBSS for 1 min. To reduce background staining, neurons were washed with 20 μM ADVASEP-7, a sulphobutylated derivative of β-cyclodextrin (Tait et al., 1992) for 1 min. ADVASEP-7 has a higher affinity for FM1-43 than plasma membranes and has been shown to greatly reduce background staining in brain slices (Kay et al., 1999). After the incubation with 10 μM TTX for 30 min, three images ([1] stained image; [2] destained image obtained after the treatment with high K^+-HBSS; and [3] differential interference contrast [DIC] image) were obtained for each microscopic field of view using confocal microscopy with a 10× objective. The second image was subtracted from the first, which revealed the presynaptic sites where depolarization-specific release had occurred (Fig. 4C, top panels). The fluorescent puncta in each microscopic field of view were counted. The number of synapses per neuron was estimated by dividing the total number of puncta by the number of neurons observed in the third (DIC) image (Fig. 4C, bottom panels).

4.8. *Western blot analysis*

Cultured neurons were washed twice with ice-cold PBS and then harvested on ice with 50 mM Tris buffer (pH 7.2) containing 1 mM EDTA, 1 mM phenylmethylsulphonyl fluoride, 1 mM leupeptin, 1 μg/ml antipain and 1 μg/ml aprotinin. After intense sonication (23 kHz, 1 min×3), the cell suspension was centrifuged at 800×*g* for 5 min at 4 °C. An

UNCORRECTED PROOF

Please cite this article as: Sato, K., et al., β-Estradiol induces synaptogenesis in the hippocampus by enhancing brain-derived neurotrophic factor release from dentate gyrus granule cells, Brain Res. (2007), doi:10.1016/j.brainres.2007.02.093

aliquot of this supernatant was removed for the protein assay. Another aliquot was diluted in SDS sample buffer. Protein samples containing an equal amount of protein were separated by electrophoresis on 10% polyacrylamide-SDS gels and transferred onto polyvinyliden difluoride membranes in 49.6 mM Tris, 384 mM glycine and 0.01% (wt/vol) SDS at 30 V overnight followed by 80 V for 1 h. The membranes were incubated with Tris-buffered saline (TBS) containing 0.1% (vol/vol) Tween 20, 5% (wt/vol) skim milk, 2% (wt/vol) BSA, and 0.1% (wt/vol) sodium azide for 1 h, followed by overnight incubation with protein A purified rabbit anti-BDNF polyclonal antibody (AB1534SP, Chemicon) (1:1000) or rabbit polyclonal IgG to β-actin (1:1000) at 4 °C. After washing (30 min), the membranes were then incubated with peroxidase-conjugated anti-rabbit IgG (1:1000) for 1 h at room temperature. Immunoreactive bands were visualized using the ECL kit. Optical densities (ODs) of immunoreactive bands were measured based on a gray scale of 0–256 arbitrary units. Background was subtracted from the OD and this corrected value was normalized to the corrected value of the β-actin band obtained from the same sample.

4.9. *ELISA detection of BDNF*

In comparison of BDNF contents in cultured DG neurons and cultured Ammon's horn neurons, cells were washed twice with ice-cold PBS and then harvested on ice with homogenization buffer consisting of 100 mM Trin/HCl (pH7), containing 2% (wt/vol) BSA, 1 M NaCl, 4 mM EDTA.Na2, 2% (vol/vol) Triton X-100, 0.1% (wt/vol) sodium azide, 5 μg/ml aprotinin, 0.5 μg/ml antipain, 157 μg/ml benzamidine, 0.1 μg/ml pepstatin A and 17 μg/ml phenylmethyl–sulphonyl fluoride. After intense sonication (23 kHz, 1 min×3), the homogenates are centrifuged at 14,000×*g* for 30 min. An aliquot of this supernatant was removed for the protein assay. Another aliquot was subjected to the calculation of BDNF concentration by the Chemikine BDNF sandwich ELISA kit. The plates, which were pre-coated with monoclonal antibodies against BDNF, were incubated with 100 μl of supernatant in each well overnight, followed by incubation with the secondary antibody for 3 h and color developing procedures for 1 h. Immediately after the stop solution included in the kit was added, the ODs of 450 nm were measured. A standard curve was run for each plate and linearity was confirmed for all detections. Because the lower detection limit of the kit is 7.8 pg/ml, we used data from the experiments in which the control value was higher than this limit. The concentration of BDNF was normalized to the total amount of protein. In the calculation of BDNF contents in the culture media, the culture media were collected after 10 h of incubation with E2, centrifuged at 1500×*g*, and the concentration of BDNF in the supernatants was determined by ELISA. Because in this case the values of the control group varied from experiment to experiment by several folds, we set 'basal value' in each experiment. 24 h after medium change, BDNF concentrations in the culture media were calculated and averaged for 4 wells in one experiment. This value was taken as the 'basal value' and the data were normalized to this 'basal value' in each experiment.

4.10. *Drug treatment*

E2 was dissolved at 100 mM in ethanol and diluted to the final concentrations with the culture medium. For PSD95 immunohistochemistry and FM1-43 analysis, cultured slices and cells were treated with various concentrations of E2 for 24 h. ICI (Ki: 1.5 nM for ERα, 6.4 nM for ERβ; Kuiper et al., 1997) was dissolved at 1 mM in ethanol and co-applied at 1 μM with E2. K252a (Squinto et al., 1991; Bothwell, 1995) was dissolved at 1 mM in DMSO and co-applied at 200 nM with E2. This concentration completely blocks the effect of BDNF in cultured hippocampal slices (Koyama et al., 2004). BDNFAB (protein A purified sheep anti-BDNF polyclonal antibody, AB1513SP, Chemicon) was dissolved in the culture medium at 10 μg/ml. This concentration blocks the effect of endogenous BDNF (Rasika et al., 1999; Matsunaga et al., 2004). For ELISA detection of the released BDNF, cultured cells were treated with E2 for 10 h. KT5720 (Ki: 56 nM [Kase et al., 1987]) was dissolved in the ethanol at 1 mM and co-applied at 200 nM with E2. Rp-cAMP (Ki: 11 μM; Rothermel and Parker Botelho, 1988) was dissolved in PBS at 10 mM and co-applied at 10 μM with E2. U0126 (Ki: 72 nM for MEK1, 58 nM for MEK2; Duncia et al., 1998) was dissolved in DMSO at 10 mM and co-applied at 10 μM with E2. We also confirmed beforehand that 0.1% ethanol or 0.1% DMSO (the maximal concentration used for vehicle in our experiments) alone had no effects in cultured hippocampal slices and subregional hippocampal neuron cultures (Fig. S1).

4.11. *Data analysis*

All data regarding the expression level of PSD95, the spine density, and the number of FM1-43 positive puncta, were quantified in a blinded manner. For quantification of PSD-95 signals, the fluorescence intensities in the synaptic sites were averaged for 4 slices in one experiment. These values were then averaged for 8 independent experiments (separate platings), and statistical analysis was performed using one-way repeated-measure analysis of variance (ANOVA) and the post hoc Tukey's test for multiple pairwise comparisons. Data are shown as the values normalized to that of CA1SR in the control group. The spine densities (the number of spines per μm of dendrite) averaged for 8 to 10 neurons per slice were averaged for 4 slices in 1 experiment. These values were then averaged for 8 independent experiments (separate platings) and statistical analysis was performed using the Student's *t* test. For FM1-43 analysis, the numbers of presynaptic sites (per neuron) were averaged for 4 wells in 1 experiment. These values were then averaged for 8 independent experiments (separate platings) and statistical analysis was performed using the Student's *t* test. In multiple pharmacological treatments, data were collected according to the methods described above, and statistical analysis was performed by one-way repeated-measure ANOVA and the post hoc Tukey's test for multiple pairwise comparisons. Data were shown as the values normalized to that of the control group. For ELISA detection of BDNF expression, the normalized values (BDNF/total protein) were averaged for 4 wells in one experiment. These values were then averaged for 4 independent experiments (separate platings), and statistical analysis was

UNCORRECTED PROOF

Please cite this article as: Sato, K., et al., β-Estradiol induces synaptogenesis in the hippocampus by enhancing brain-derived neurotrophic factor release from dentate gyrus granule cells, Brain Res. (2007), doi:10.1016/j.brainres.2007.02.093

performed by one-way repeated-measure ANOVA and the post hoc Tukey's test for multiple pairwise comparisons. For ELISA detection of the released BDNF, the values normalized to the basal value were averaged for 4 wells in one experiment. These values were then averaged for 4 independent experiments (separate platings), and statistical analysis was performed using one-way repeated-measure ANOVA and the post-hoc Tukey's test for multiple pairwise comparisons. Values of $p<0.05$ were considered significant.

Acknowledgments

This work was partly supported by a Grant-in-Aid for Young Scientists from the Ministry of Education, Science, Sports and Culture, Japan (KAKENHI 18700373), and a grant for Health Science Research Including Drug Innovation from the Japan Health Sciences Foundation awarded to K.S.; Health and Labour Science Research Grants for Research on Advanced Medical Technology from the Ministry of Health, Labour and Welfare, Japan, and a Grant-in-Aid for Scientific Research from the Ministry of Education, Science, Sports and Culture, Japan (KAKENHI 13672319), awarded to K.N.

Appendix A. Supplementary data

Supplementary data associated with this article can be found, in the online version, at doi:10.1016/j.brainres.2007.02.093.

REFERENCES

Acsady, L., Kamondi, A., Sik, A., Freund, T., Buzsaki, G., 1998. GABAergic cells are the major postsynaptic targets of mossy fibers in the rat hippocampus. J. Neurosci. 18, 3386–3403.

Aguado, F., Carmona, M.A., Pozas, E., Aguilo, A., Martinez-Guijarro, F.G., Alcantara, S., Borrell, V., Yuste, R., Ibanez, C.F., Soriano, E., 2003. BDNF regulates spontaneous correlated activity at early developmental stages by increasing synaptogenesis and expression of the K+/Cl– co-transporter KCC2. Development 130, 1267–1280.

Alsina, B., Vu, T., Cohen-Cory, S., 2001. Visualizing synapse formation in arborizing optic axons in vivo: dynamics and modulation by BDNF. Nat. Neurosci. 4, 1093–1101.

Balkowiec, A., Katz, D.M., 2002. Cellular mechanisms regulating activity-dependent release of native brain-derived neurotrophic factor from hippocampal neurons. J. Neurosci. 22, 10399–10407.

Beyer, C., Karolczak, M., 2000. Estrogenic stimulation of neurite growth in midbrain dopaminergic neurons depends on cAMP/protein kinase A signaling. J. Neurosci. Res. 59, 107–116.

Beyer, C., Ivanova, T., Karolczak, M., Kuppers, E., 2002. Cell type-specificity of nonclassical estrogen signaling in the developing midbrain. J. Steroid Biochem. Mol. Biol. 81, 319–325.

Beyer, C., Pawlak, J., Karolczak, M., 2003. Membrane receptors for oestrogen in the brain. J. Neurochem. 87, 545–550.

Bothwell, M., 1995. Functional interactions of neurotrophins and neurotrophins receptors. Annu. Rev. Neurosci. 18, 223–253.

Cambiasso, M.J., Carrer, H.F., 2001. Nongenomic mechanism mediates estradiol stimulation of axon growth in male rat hypothalamic neurons in vitro. J. Neurosci. Res. 66, 475–481.

Clarke, C.H., Norfleet, A.M., Clarke, M.S., Watson, C.S., 2000. Perimembrane localization of the estrogen receptor (protein in neuronal processes of cultured hippocampal neurons. Neuroendocrinology 71, 34–42.

Cochilla, A.J., Angleson, J.K., Betz, W.J., 1999. Monitoring secretory membrane with FM1-43 fluorescence. Ann. Rev. Neurosci. 22, 1–10.

Craven, S.D., Bredt, D.S., 1998. PDZ proteins organize synaptic signaling pathways. Cell 93, 495–509.

Danzer, S.C., McNamara, J.O., 2004. Localization of brain-derived neurotrophic factor to distinct terminals of mossy fiber axons implies regulation of both excitation and feedforward inhibition of CA3 pyramidal cells. J. Neurosci. 24, 11346–11355.

De Simoni, A., Griesinger, C.B., Edwards, F.A., 2003. Development of rat CA1 neurones in acute versus organotypic slices: role of experience in synaptic morphology and activity. J. Physiol. 550 (Pt. 1), 135–147.

Dieni, S., Rees, S., 2002. Distribution of brain-derived neurotrophic factor and TrkB receptor proteins in the fetal and postnatal hippocampus and cerebellum of the guinea pig. J. Comp. Neurol. 454, 229–240.

Duncia, J.V., Santella III, J.B., Higley, C.A., Pitts, W.J., Wityak, J., Frietze, W.E., Rankin, F.W., Sun, J.H., Earl, R.A., Tabaka, A.C., Teleha, C.A., Blom, K.F., Favata, M.F., Manos, E.J., Daulerio, A.J., Stradley, D.A., Horiuchi, K., Copeland, R.A., Scherle, P.A., Trzaskos, J.M., Magolda, R.L., Trainor, G.L., Wexler, R.R., Hobbs, F.W., Olson, R.E., 1998. MEK inhibitors: the chemistry and biological activity of U0126, its analogs, and cyclization products. Bioorg. Med. Chem. Lett. 8 (20), 2839–2844.

Garner, C.C., Nash, J., Huganir, R.L., 2000. PDZ domains in synapse assembly and signaling. Trends Cell Biol. 10, 274–280.

Gartner, A., Staiger, V., 2002. Neurotrophin secretion from hippocampal neurons evoked by long-term-potentiation-inducing electrical stimulation patterns. Proc. Natl. Acad. Sci. U. S. A. 99 (9), 6386–6391.

Germain, S.J., Campbell, P.S., Anderson, J.N., 1978. Role of the serum estrogen-binding protein in the control of tissue estradiol levels during postnatal development of the female rat. Endocrinology 103, 1401–1410.

Gould, E., Woolley, C.S., Frankfurt, M., McEwen, B.S., 1990. Gonadal steroids regulate dendritic spine density in hippocampal pyramidal cells in adulthood. J. Neurosci. 10, 1286–1291.

Hartmann, M., Heumann, R., Lessmann, V., 2001. Synaptic secretion of BDNF after high frequency stimulation of glutamatergic synapses. EMBO J. 20, 5887–5897.

Haubensak, W., Narz, F., Heumann, R., Lessmann, V., 1998. BDNF-GFP containing secretory granules are localized in the vicinity of synaptic junctions of cultured cortical neurons. J. Cell Sci. 111, 1483–1493.

Hojo, Y., Hattori, T., Enami, T.A., Hurukawa, A., Suzuki, K., Ishii, H.T., Mukai, H., Morrison, J.H., Janssen, W.G., Kominami, S., Harada, N., Kimoto, T., Kawato, S., 2004. Adult male rat hippocampus synthesizes estradiol from pregnenolone by cytochromes P45017α and P450 aromatase localized in neurons. Proc. Natl. Acad. Sci. U. S. A. 101, 865–870.

Ikegaya, Y., Nishiyama, N., Matsuki, N., 2000. L-type Ca^{2+} channel blocker inhibits mossy fiber sprouting and cognitive deficits following pilocarpine seizures in immature mice. Neuroscience 98, 647–659.

Ivanova, T., Kuppers, E., Engele, J., Beyer, C., 2001. Estrogen stimulates brain-derived neurotrophic factor expression in embryonic mouse midbrain neurons through a membrane-mediated and calcium-dependent mechanism. J. Neurosci. Res. 66, 221–230.

Jontes, J.D., Smith, S.J., 2000. Filopodia, spines, and the generation of synaptic diversity. Neuron 27, 11–14.

Kase, H., Iwahashi, K., Nakanishi, S., Matsuda, Y., Yamada, K., Takahashi, M., Murakata, C., Sato, A., Kaneko, M., 1987. K-252 compounds, novel and potent inhibitors of protein kinase C

UNCORRECTED PROOF

and cyclic nucleotide-dependent protein kinases. Biochem. Biophys. Res. Commun. 142, 436–440.
Kay, A.R., Alfonso, A., Alford, S., Cline, H.T., Holgado, A.M., Sakmann, B., Snitsarev, V.A., Stricker, T.P., Takahashi, M., Wu, L.G., 1999. Imaging synaptic activity in intact brain and slices with FM1-43 in *C. elegans*, lamprey, and rat. Neuron 24, 809–817.
Kelly, M.J., Levin, E.R., 2001. Rapid actions of plasma membrane estrogen receptors. Trends Endocrinol. Metab. 12, 152–156.
Koyama, R., Yamada, M.K., Fujisawa, S., Katoh-Semba, R., Matsuki, N., Ikegaya, Y., 2004. Brain-derived neurotrophic factor induces hyperexcitable reentrant circuits in the dentate gyrus. J. Neurosci. 24, 7215–7224.
Kramar, E.A., Lin, B., Lin, C.Y., Arai, A.C., Gall, C.M., Lynch, G., 2004. A novel mechanism for the facilitation of theta-induced long-term potentiation by brain-derived neurotrophic factor. J. Neurosci. 24 (22), 5151–5161.
Kretz, O., Fester, L., Wehrenberg, U., Zhou, L., Brauckmann, S., Zhao, S., Prange-Kiel, J., Naumann, T., Jarry, H., Frotscher, M., Rune, G.M., 2004. Hippocampal synapses depend on hippocampal estrogen synthesis. J. Neurosci. 24, 5913–5921.
Kuiper, G.G., Carlsson, B., Grandien, K., Enmark, E., Haggblad, J., Nilsson, S., Gustafsson, J.A., 1997. Comparison of the ligand binding specificity and transcript tissue distribution of estrogen receptors alpha and beta. Endocrinology 138, 863–870.
Lawrence, J.J., McBain, C.J., 2003. Interneuron diversity series: containing the detonation-feedforward inhibition in the CA3 hippocampus. Trends Neurosci. 26, 631–640.
Lessmann, V., Gottmann, K., Malcangio, M., 2003. Neurotrophin secretion: current facts and future prospects. Prog. Neurobiol. 69, 341–374.
Matsunaga, W., Shirokawa, T., Isobe, S., 2004. BDNF is necessary for maintenance of noradrenergic innervations in the aged rat brain. Neurobiol. Aging 25, 341–348.
McAllister, A.K., Katz, L.C., Lo, D.C., 1999. Neurotrophins and synaptic plasticity. Annu. Rev. Neurosci. 22, 295–318.
McEwen, B., Akama, K., Alves, S., Brake, W.G., Bulloch, K., Lee, S., Li, C., Yuen, G., Milner, T.A., 2001. Tracking the estrogen receptor in neuron: implication for estrogen-induced synapse formation. Proc. Natl. Acad. Sci. U. S. A. 98, 7093–7100.
Mizuhashi, S., Nishiyama, N., Matsuki, N., Ikegaya, Y., 2001. Cyclic nucleotide-mediated regulation of hippocampal mossy fiber development: a target-specific guidance. J. Neurosci. 15 21 (16), 6181–6194.
Murphy, D.D., Cole, N.B., Greenberger, V., Segal, M., 1998a. Estradiol increases dendritic spine density by reducing GABA neurotransmission in hippocampal neurons. J. Neurosci. 18 (7), 2550–2559.
Murphy, D.D., Cole, N.B., Segal, M., 1998b. Brain-derived neurotrophic factor mediates estradiol-induced dendritic spine formation in hippocampal neurons. Proc. Natl. Acad. Sci. U. S. A. 95 (19), 11412–11417.
Nakagami, Y., Saito, H., Matsuki, N., 1997. The regional vulnerability to blockade of action potentials in organotypic hippocampal culture. Brain Res. Dev. Brain Res. 103 (1), 99–102.
Okabe, S., Miwa, A., Okado, H., 2001. Spine formation and correlated assembly of presynaptic and postsynaptic molecules. J. Neurosci. 21, 6105–6114.
Patterson, S.L., Pittenger, C., Morozov, A., Martin, K.C., Scanlin, H., Drake, C., Kandel, E.R., 2001. Some forms of cAMP-mediated long-lasting potentiation are associated with release of BDNF and nuclear translocation of phospho-MAP kinase. Neuron 32, 123–140.
Pozzo-Miller, L.D., Inoue, T., Murphy, D.D., 1999. Estradiol increases spine density and NMDA-dependent Ca^{2+} transients in spines of CA1 pyramidal neurons from hippocampal slices. J. Neurophysiol. 81, 1404–1411.
Qin, L., Marrs, G.S., Mckim, R., Dailey, M.E., 2001. Hippocampal mossy fibers induce assembly and clustering of PSD95-containing postsynaptic densities independent of glutamate receptor activation. J. Comp. Neurol. 440, 284–298.
Rasika, S., Alvarez-Buylla, A., Nottebohm, F., 1999. BDNF mediates the effects of testosterone on the survival of new neurons in an adult brain. Neuron 22, 53–62.
Razandi, M., Pedram, A., Merchenthaler, I., Greene, G.L., Levin, E.R., 2004. Plasma membrane estrogen receptors exist and functions as dimmers. Mol. Endocrinol. 18, 2854–2865.
Rothermel, J.D., Parker Botelho, L.H., 1988. A mechanistic and kinetic analysis of the interactions of the diastereoisomers of adenosine 3′,5′-(cyclic)phosphorothioate with purified cyclic AMP-dependent protein kinase. Biochem. J. 251, 757A–762A.
Sato, K., Matsuki, N., Ohno, Y., Nakazawa, K., 2002. Effects of 17β-estradiol and xenoestrogens on the neuronal survival in an organotypic hippocampal culture. Neuroendocrinology 76, 223–234.
Scharfman, H.E., MacLusky, N.J., 2005. Similarities between actions of estrogen and BDNF in the hippocampus: coincidence or clue? Trends Neurosci. 28 (2), 79–85.
Scharfman, H.E., Mercurio, T.C., Goodman, J.H., Wilson, M.A., MacLusky, N.J., 2003. Hippocampal excitability increases during the estrous cycle in the rat: a potential role for brain-derived neurotrophic factor. J. Neurosci. 23, 11641–11652.
Segal, M., Murphy, D., 2001. Estradiol induces formation of dendritic spines in hippocampal neurons: functional correlates. Horm. Behav. 40 (2), 156–159.
Segars, J.H., Driggers, P.H., 2002. Estrogen action and cytoplasmic signaling cascades. Part I: membrane-associated signaling complexes. Trends Endocrinol. Metab. 13, 349–354.
Seil, F.J., Drake-Baumann, R., 2000. TrkB receptor ligands promote activity-dependent inhibitory synaptogenesis. J. Neurosci. 20, 5367–5373.
Sohrabji, F., Miranda, R.C., Toran-Allerand, C.D., 1995. Identification of a putative estrogen response element in the gene encoding brain-derived neurotrophic factor. Proc. Natl. Acad. Sci. U. S. A. 92, 11110–11114.
Squinto, S.P., Stitt, T.N., Aldrich, T.H., Davis, S., Bianco, S.M., Radziejewski, C., Glass, D.J., Masiakowski, P., Furth, M.E., Valenzuela, D.M., Distefano, P.S., Yancopolous, G.D., 1991. trkB encodes a functional receptor for brain-derived neurotrophic factor and neurotrophin-3 but not nerve growth factor. Cell 65, 885–893.
Tait, R.J., Skanchy, D.J., Thompson, D.P., Chetwyn, N.C., Dunshee, D.A., Rajewski, R.A., Stella, V.J., Stobaugh, J.F., 1992. Characterization of sulfoalkyl ether derivatives of beta-cyclodextrin by capillary electrophoresis with indirect UV detection. J. Pharm. Biomed. Anal. 10, 615–622.
Takahashi, H., Sekino, Y., Tanaka, S., Mizui, T., Kishi, S., Shirao, T., 2003. Drebrin-dependent actin clustering in dendritic filopodia governs synaptic targeting of postsynaptic density-95 and dendritic spine morphogenesis. J. Neurosci. 23, 6586–6595.
Tanapat, P., Hastings, N.B., Reeves, A.J., Gould, E., 1999. Estrogen stimulates a transient increase in the number of new neurons in the dentate gyrus of the adult female rat. J. Neurosci. 19 (14), 5792–5801.
Thomas, P., Pang, Y., Filardo, E.J., Dong, J., 2004. Identity of an estrogen membrane receptor coupled to a G-protein in human breast cancer cells. Endocrinology 146, 624–632.
Toran-Allerand, C.D., Guan, X., MacLusky, N.J., Horvath, T.L., Diano, S., Singh, M., Connolly Jr., E.S., Nethrapalli, I.S., Tinnikov, A.A., 2002. ER-X: a novel, plasma membrane-associated, putative estrogen receptor that is regulated during development and after ischemic brain injury. J. Neurosci. 22, 8391–8401.
Tyler, W.J., Alonso, M., Bramham, C.R., Pozzo-Miller, L.D., 2002. From acquisition to consolidation: on the role of brain-derived neurotrophic factor signaling in hippocampal-dependent learning. Learn. Mem. 9 (5), 224–237.
Woolley, C.S., 1998. Estrogen-mediated structural and functional

UNCORRECTED

Please cite this article as: Sato, K., et al., β-Estradiol induces synaptogenesis in the hippocampus by enhancing brain-derived neurotrophic factor release from dentate gyrus granule cells, Brain Res. (2007), doi:10.1016/j.brainres.2007.02.093

synaptic plasticity in the female rat hippocampus. Horm. Behav. 34 (2), 140–148.
Woolley, C.S., Schwartzkroin, P.A., 1998. Hormonal effects on the brain. Epilepsia 39 (Suppl. 8), S2–S8.
Wu, Y.J., Kruttgen, A., Moller, J.C., Shine, D., Chan, J.R., Shooter, E.M., Cosgaya, J.M., 2004. Nerve growth factor, brain-derived neurotrophic factor, and neurotrophin-3 are sorted to dense-core vesicles and released via the regulated pathway in primary rat cortical neurons. J. Neurosci. Res. 75, 825–834.
Znamensky, V., Akama, K.T., McEwen, B., Milner, T., 2003. Estrogen levels regulate the subcellular distribution of phosphorylated Akt in hippocampal CA1 dendrites. J. Neurosci. 23, 2340–2347.

UNCORRECTED PROOF

Please cite this article as: Sato, K., et al., β-Estradiol induces synaptogenesis in the hippocampus by enhancing brain-derived neurotrophic factor release from dentate gyrus granule cells, Brain Res. (2007), doi:10.1016/j.brainres.2007.02.093

Available online at www.sciencedirect.com
ScienceDirect
Toxicology in Vitro 21 (2007) 521–526
Toxicology in Vitro
www.elsevier.com/locate/toxinvit

Two-dimensional electrophoresis of protein from cultured postimplantation rat embryos for developmental toxicity studies

Makoto Usami [a,*], Katsuyoshi Mitsunaga [b], Ken Nakazawa [a]

[a] *Division of Pharmacology, National Institute of Health Sciences, 1-18-1, Kamiyoga, Setagaya, Tokyo 158-8501, Japan*
[b] *School of Pharmaceutical Sciences, Toho University, Japan*

Received 6 January 2006; accepted 10 November 2006
Available online 17 November 2006

Abstract

A simple method for two-dimensional electrophoresis (2-DE) of rat embryonic protein was described. Rat embryos cultured for 24 h from day 10.5 of gestation were used as protein samples. Protein samples were lysed in rehydration buffer and separated by isoelectric focusing with immobilized pH gradient for the first dimension and by sodium dodecyl sulfate–polyacrylamide gel electrophoresis for the second dimension. The use of the DeStreak Reagent as an antioxidant in the lysis buffer and electrode pads in the isoelectric focusing greatly improved the 2-DE pattern. When an embryo was used as a protein sample, about 800 protein spots were detected by silver staining in a 2-DE gel of the standard format. Eighty-one protein spots were identified by mass spectrometry for a primary 2-DE map. The same method could be applied to yolk sac membranes from the cultured embryos. The present method was considered to be suitable for a concomitant 2-DE analysis in in vitro developmental toxicity studies.
© 2006 Elsevier Ltd. All rights reserved.

Keywords: Two-dimensional electrophoresis; Rat; Embryo; Yolk sac; Developmental toxicity; Proteome

1. Introduction

Recent advances in two-dimensional electrophoresis (2-DE) made it possible to analyze the changes in protein expression pattern caused by exogenous stimulations in various tissues, such as the liver (Fountoulakis et al., 2000), kidney (Xu et al., 2005) and blood components (Piubelli et al., 2005). In developmental toxicity studies, the analysis of embryonic protein expression pattern by 2-DE is considered to be useful for the mechanism-based evaluation of developmental toxicants.

On the other hand, it is expected that the cultured rat embryos can be better protein samples for the analysis of protein expression pattern in developmental toxicity studies. Postimplantation rat embryo culture is now widely used in developmental toxicity studies, by which embryos can be exposed to test chemicals under controlled conditions with a small number of animals and a small amount of test chemicals (Schmid et al., 1997).

However, there have been no suitable 2-DE methods for the analysis of embryonic protein expression pattern since most methods are for radio-labeled proteins but not for total proteins (Baumgartner et al., 1994; Praxmayer et al., 1992). The standard 2-DE methods that we tried could not be applicable because of a high salt concentration and poor solubility of embryonic samples. A method reported for the proteome analysis of mouse embryos is not considered suitable for routine analysis in developmental toxicity studies because of troublesome pretreatment of embryo samples, i.e., water-wash and dry-ice freezing (Greene et al., 2002).

In the present study, we described a simple 2-DE method for the analysis of cultured postimplantation rat embryos. By our method about 800 protein spots were detected in a

Abbreviations: 2-DE, two-dimensional electrophoresis; IEF, isoelectric focusing; IPG, immobilized pH gradient; SDS, sodium dodecyl sulfate; PAGE, polyacrylamide gel electrophoresis.

* Corresponding author. Tel.: +81 3 3700 1141x342; fax: +81 3 3707 6950.
E-mail address: usami@nihs.go.jp (M. Usami).

0887-2333/$ - see front matter © 2006 Elsevier Ltd. All rights reserved.
doi:10.1016/j.tiv.2006.11.003